

# **ESTABLISHING A RELATIONSHIP BETWEEN HARDNESS AND STRENGTH OF FRICTION STIR WELDED JOINTS**

*A Project report submitted in partial fulfilment of the requirements*

*for the award of the degree of*

**Bachelor of Technology  
in  
Mechanical Engineering**

*Submitted by*

<b>V.M.G.S. SAIKIRAN</b>	<b>319126520120</b>
<b>G. JAYA PRAKASH</b>	<b>320126520L07</b>
<b>Y. JAHNAVI</b>	<b>320126520L09</b>
<b>K. NIRIKSHAN BABU</b>	<b>319126520088</b>

*Under the Esteemed Guidance of*

**Mr. D.S.S. Ravi Kiran (PhD), A.M.I.E., M.I.I.W**  
Assistant Professor



**DEPARTMENT OF MECHANICAL ENGINEERING**

**ANIL NEERUKONDA INSTITUTE OF TECHNOLOGY & SCIENCES (A)**

(Permanently Affiliated to Andhra University, Approved by AICTE, Accredited by NBA Tier-I, NAAC)

Sangivalasa, Visakhapatnam (District) Andhra Pradesh -India– 531162.


**APRIL 2023**

**DEPARTMENT OF MECHANICAL ENGINEERING**  
**ANIL NEERUKONDA INSTITUTE OF TECHNOLOGY & SCIENCES**  
**(UGC Autonomous & Permanently Affiliated to Andhra University)**



**CERTIFICATE**

This is to certify that the Project Report entitled “**Establishing a relation between hardness and strength of friction stir welded joints**” being submitted by **V.M.G.S. Saikiran (319126520120)**, **G. Jaya Prakash (320126520L07)**, **Y. Jahnavi (320126520L09)**, **K. Nirikshan Babu (319126520088)** to the Department of Mechanical Engineering, ANITS is a record of the bonafide work carried out by them under the esteemed guidance of **Mr. D.S.S. Ravi Kiran**. The results embodied in the report have not been submitted to any other University or Institute for the award of any degree or diploma.

  
**Project Guide**

**Mr. D.S.S. RAVI KIRAN**  
Assistant Professor  
Dept. of Mechanical Engineering,  
ANITS

  
**Head of the Department**

**Dr. B. NAGA RAJU**  
Professor  
Dept. of Mechanical Engineering  
ANITS

**THIS PROJECT IS APPROVED BY THE FOLLOWING BOARD OF EXAMINERS**

**INTERNAL EXAMINER**

*[Handwritten signature]*  
18.4.23

**PROFESSOR & HEAD**  
Department of Mechanical Engineering  
ANIL NEERUKONDA INSTITUTE OF TECHNOLOGY & SCIENCE  
Sangivalasa-531 162 VISAKHAPATNAM Dist. A.P.

**EXTERNAL EXAMINER**

*S. Deval*  
18/4/23

## ACKNOWLEDGEMENTS

We express our sincere thanks to our guide Mr D.S.S. RAVIKIRAN (PhD), A.M.I.I.E, M.I.I.W. ASST Professor, we thank Mr M.V.N.V Satya Narayana (PhD) of the Department of Mechanical Engineering. Anil Neerukonda Institute of Technology and Sciences, Sangivalasa, Bheemunipatnam, Visakhapatnam District, for his valuable guidance and encouragement at every stage of work. He has been a perennial source of inspiration and motivation from the project's conception until its conclusion.

We were very thankful to Prof. K. SRI RAMA KRISHNA, Principal (ANITS) and Dr. B. Nagaraju, Head of the Department, Mechanical Department. Anil Neerukonda Institute of Technology and Sciences, for his ever willingness to share his valuable knowledge and constantly inspire us through suggestions and their invaluable support and facilities.

I sincerely thank all the Staff Members of the Mechanical Engineering Department for giving us their heart and full support in completing this project work.

We sincerely thank the non-teaching staff members of the Mechanical Engineering Department for their kind cooperation and support in carrying on the work.

Finally, we like to convey our thanks to all who have contributed either directly or indirectly to the completion of this project work.

REGARDS

V.M.G.S. SAIKIRAN	319126520120
G. JAYAPRAKASH	320126520L07
Y. JAHAVI	320126520L09
K. NIRIKSHAN BABU	319126520088

## ABSTRACT

Plates of solid-state metal are joined by friction stir welding (FSW). The method was introduced in the year (1991). By combining identical and different aluminium joints and some composite alloys, the primary goal of the friction stir welding technique (FSW) is to determine the consistent relationship between tensile strength and hardness. They focused initially on the linear relationship between friction stir welding's strength and hardness under various Colling conditions. No matter the grain, aluminium alloys have additional important alloying components. It might be challenging to achieve the best outcomes using Convectional welding techniques, such as TIG/MIG welding. Therefore, a solid-state joining method, such as friction stir welding (FSW), is strongly advised to address these issues. To learn more about the properties of the weld joint and the base metals, we linked these dissimilar (AA6061-AA5083) alloys in an open atmosphere with similar AA6061 alloys using friction stir welding. Tensile testing and hardness testing were utilised for that.

**KEYWORDS:** Friction stir welding, Aluminium Alloys, dissimilar welding, composites, Ultimate tensile strength, Yield strength, Vickers microhardness.

## **TABLE OF CONTENTS**

<b>DESCRIPTION</b>	<b>PAGE NO.</b>
<b>ACKNOWLEDGEMENT</b>	iii
<b>ABSTRACT</b>	iv
<b>TABLE OF CONTENTS</b>	v
<b>LIST OF TABLES</b>	vii
<b>LIST OF FIGURES</b>	viii
<b>NOMENCLATURE</b>	x
<b>CHAPTER 1: INTRODUCTION</b>	<b>1</b>
1.1 Background	1
1.2 Working principle	2
1.3 Research Objectives and Approach	3
1.4 Framework of the Thesis	3
1.5 Friction Stir Welding	4
1.6 Working of Friction Stir Welding	6
1.7 Aluminum (Al)	7
1.8 Applications	8
1.9 Need of Aluminum (Al)	9
1.10 Aluminum used	10
1.10.1 Aluminum Alloy – 6061	10
1.10.2 Aluminum Alloy – 5083	10
1.11 Microstructural development in FSW	11
1.12 Material Flow in FSW	13
1.13 Microstructure evolution of FSW	15
1.14 Materials used for the tool	17
1.14.1 Tool Materials	19
1.15 Defects in FSW	20
1.16 Application of FSW	22

<b>CHAPTER 2:</b>	<b>LITERATURE REVIEW</b>	<b>23</b>
2.2	Objectives	26
<b>CHAPTER 3:</b>	<b>MATERIALS AND METHODOLOGY</b>	<b>28</b>
3.1	Materials	28
3.2	Friction stir welding	28
3.2.1	FSW machine	29
3.2.2	Mechanical testing	30
3.2.3	Tool used for FSW	32
3.2.4	Tool parameter	33
3.3	Hardness test	33
3.4	Tensile test	34
3.4.1	Specifications of Tensile Testing Machine	35
<b>CHAPTER 4:</b>	<b>RESULTS AND DISCUSSIONS</b>	<b>36</b>
<b>CHAPTER 5:</b>	<b>CONCLUSION</b>	<b>61</b>
<b>CHAPTER 6:</b>	<b>REFERENCES</b>	<b>62</b>

## **LIST OF TABLES**

<b>Table No.</b>	<b>Title of the Table</b>	<b>Page No.</b>
1.1	Major benefits of FSW	6
1.2	The United States revised the designation system for aluminium-cast Alloys	10
1.3	Common types of defects observed in FSW	21
3.1	Specification of 4axis friction stir welding	31
4.1	UTS YS HV values obtained from AA6061-5083 FSW joint	37
4.2	UTS YS HV values obtained from AA6061-5083 (2) FSW joint	39
4.3	UTS YS HV values obtained from AA6061 similar FSW joints	41
4.4	UTS and HV values obtained from FSW of similar AA1200	43
4.5	UTS and HV values obtained from FSW of similar AA1200 (2)	44
4.6	UTS and HV values obtained from FSW of similar AA1200 (TCT)	45
4.7	UTS and HV values obtained from FSW of similar FSW joints	46
4.8	UTS and HV values obtained from FSW of similar AA6061-T6 FSW joint	47
4.9	UTS and HV values obtained from FSW of AA6061-T6-AA7075-T6(800rpm)	49
4.10	UTS and HV values obtained from AA6061-7075 FSW joints(900rpm)	50
4.11	UTS and HV values obtained from AA6061-7039 FSW dissimilar joints	51
4.12	UTS and HV values obtained from AA2014-7075 FSW dissimilar joint	52
4.13	UTS and HV values obtained from AA6061T6-AA7075T6	53



	FSW joints	
4.14	UTS YS HV values obtained from AA6061-T6 alloy surface Hybrid Composites	55
4.15	UTS vs HV graph of aluminium composites via FSW	.56
4.16	UTS vs HV graphs of composite reinforced FSW joint	57
4.17	UTS vs HV graph of aluminium composites FSW joint	58
4.18	UTS vs HV graph of surface hybrid aluminium composites	59

### **LIST OF FIGURES :**

1.1	Schematic illustration of friction stir welding	3
1.2	Schematic process of FSW	05
1.2.1	FSW process in action	07
1.2.2	Tool heated due to friction	07
1.3	Aluminium metal element	08
1.4(a)	Macrostructure of the friction-stir welded 6061-T6 Al alloy	11
1.4(b)	Microstructure of the dynamic recrystallized zone (DXZ) thermo-mechanically affected zone (TMAZ), heat-affected zone (HAZ) and initial base material (BM) taken at yellow square marks shown	12
1.5	Two modes of metal transfer phenomenon	14
1.6	FSW on similar Aluminum alloys	18
1.7	Characteristics flaw types in friction stir welding	20
3.1 (a)	FSW schematic illustration	28
3.1 (b)	FSW tool with dimensions	28
3.2	FRICION STIR WELDING MACHINE	29
3.3	Control system	30

3.3 (a)	Friction Stir Processing with a Tool	32
3.3 (b)	Fixture Setup	32
3.4	FSW process on dissimilar Aluminum alloys	32
3.5	Hardness Test Process	33
3.6	Hardness testing machine	34
3.7	B- Scale indicator	34
3.8	Universal Testing Machine (UTM)	35
4.1a	UTS vs HV between AA6061- AA5083 FSW welded joints	37
4.1b	YS vs HV graph of AA6061-AA5083 welded joints	38
4.2a	UTS vs HV graph of AA6061-5083 welded joints	39
4.2b	YS vs HV graph of AA6061-5083 welded joints	40
4.3a	UTS vs HV graph of AA6061 similar joints	41
4.3b	YS vs HV graph of AA6061 similar joints	42
4.4	UTS vs HV graph of AA1200 similar FSW welded joint	43
4.5	UTS vs HV graph of similar AA1200 FSW welded joint	44
4.6	UTS vs HV graph of similar AA1200 FSW weld joint with cylindrical Tool with groove	45
4.7	UTS vs HV graph of similar FSW welded joint	46
4.8	UTS vs HV graph of similar AA60601-T6 FSW joint	47
4.9	UTS vs HV graph obtained from dissimilar AA6061-AA7075 FSW joint	49
4.10	UTS vs HV graph of dissimilar AA6061-AA7075 FSW joint	50
4.11	UTS vs HV graph of dissimilar AA6061-7039 FSW joint	51
4.12	UTS vs HV graph of dissimilar AA2014-AA7075 FSW joint	52
4.13	UTS vs HV graph of dissimilar AA6061T6 – 7075T6 FSW joint	.53
4.14	UTS vs HV graph of composite welded joint of similar AA6061 FSW joints	55

4.15	UTS vs HV graph of aluminium composites via FSW	56
4.16	UTS vs HV graphs of composite reinforced FSW joint	57
4.17	UTS vs HV graph of aluminium composites FSW joint	58
4.18	UTS vs HV graph of surface hybrid aluminium composites	59

## **NOMENCLATURE**

1. FSW - Friction Stir Welding
2. TIG - Tungsten Inert Gas
3. MIG - Metal Inert Gas
4. AMMC - Aluminum Metal-Matrix Composites
5. AA - Aluminum Alloy
6. HSS – High-Speed Steel
7. HCP - Hexagonal Close Packed metals
8. UV – Ultraviolet
9. TMAZ - Thermomechanical Affected Zone
10. HAZ - Heat Affected Zone
11. DXZ - Dynamic Recrystallized Zone
12. BM - Base Metal
13. CDRX - Continuous dynamic recrystallisation
14. DDRX - Discontinuous dynamic recrystallisation
15. GDRX - Geometric dynamic recrystallisation
16. DRV - Dynamic recovery
17. PCBN - Poly Crystalline Boron Nitride
18. UFSW - Underwater Friction Stir Welding
19. SFSW - Submerged Friction Stir Welding
20. RS - Retreating Side
21. AS - Advancing Side
22. ANN - Artificial Neural Networks
23. SZ – Stir Zone
24. EBSD - Electron Back Scattered Diffraction
25. CFSW - Continuous Fillet Stir Welding
26. PD - Plunging Depth

27. PWHT - Post-weld heat treatment
28. UTS - Ultimate Tensile Strength
29. YS - Yield Strength
30. CNC - Computer Numerical Control
31. UTM - Universal Testing Machine
32. HV - Vickers hardness
33.  $n$  - Strain hardening coefficient
34.  $\sigma_Y$  - Yield strength
35.  $\sigma_{UTS}$  - Ultimate tensile strength
36.  $Q$  - Activation energy for lattice diffusion
37.  $\dot{\epsilon}$  - Strain rate
38.  $Z$  - Sub grain size for a given temperature and strain rate
39.  $R$  - Zener-Holloman parameter
40.  $\rho_m$  - Mobile dislocation density
41.  $\gamma_{gb}$  - Grain boundary energy
42.  $K$  - Constant fraction of the dislocation line energy that is stored in the newly formed grains
43.  $L$  - Mean slip distance of dislocations in these grains
44.  $M$  - Boundary mobility
45.  $G$  - Shear modulus
46.  $B$  - Burgers vector
47.  $d_0$  - Initial grain size

# CHAPTER 1

## INTRODUCTION

### 1.1 BACKGROUND

Friction stir welding(FSW) is one of the more promising surface modification technologies for the fine grain size structure in metals, alloys, and composites. The primary uses for FSW are in the manufacturing industry. Enhancing the mechanical and metallurgical qualities is the FSW's key benefit. Our work investigated the effects of mechanical characteristics and microstructure on both weld processes when welding two similar and dissimilar aluminium alloys in an open environment. The energy needed to melt the workpieces and, if necessary, the filler is provided by this arc.

Due to their high thermal conductivity, it has been shown that the weld penetration for Al alloys remained relatively shallow, measuring less than 3mm in a single pass. A considerable microstructural evolution is induced by the extreme temperatures and fusion welding procedures, particularly concerning hardening precipitates. Therefore, we favour FSW, a solid-state joining technique invented by The Welding Institute (TWI)[1], the U.K., in 1991, for combining light metals. A revolving hard steel pin with a cylindrical shoulder extended is advanced between two contacting metal plates in this operation.

Frictional heating is created by rubbing the spinning shoulder against the two workpieces while the rotating pin deforms the heated material. There is minimal to no porosity or other problems associated with fusion welding procedures compared to fusion welding. Considering the decreased heat input of the solid-state joining method and the high stability of hardening particles, the industrial objective of this study is to assess the potential benefits of FSW comparison to TIG and MIG.

Lightweight aluminium alloys are extensively employed in industries including aerospace and transportation (ship panels, high-speed rail frames, and vehicle components). Features of the friction stir-welded joints for simple artificial ageing. Compared to mechanical fastening together, the joints produced by FSW are less expensive and lighter. However, conventional welding techniques have several drawbacks when used on Al alloys. The metal becomes brittle, has hot cracking, and breaks easily due to the decreased strength and lack of response to future heat treatments. To avoid these problems, we employ the FSW. This paper's primary goal is to

demonstrate how friction welding of metals and composites affects the relationship between strength and hardness.

During fusion welding, Al alloys experience hot cracking, form distortion, precipitated settlement, and reduction of work hardening. Although FSW may be a possibility, the melting point of the oxide-formed aluminium is higher than the base metal itself because of the ability to weld aluminium alloys while welding. High heat conductivity is also mentioned as a cause (and is used to imply that both standards must be met), which needs to be fixed because it contributes to poor weldability.

Friction stir welding varies based on the materials' as-received state. Due to the breakdown of strengthening precipitates, For heat-treatable Al alloys, FSW processing creates a softened patch within the weld region. Al alloys that cannot be heated do not soften because they cannot undergo strain hardening. Aluminium alloys are vulnerable to strain stiffening and cannot be heated, displaying weakening in the welding area due to lower dislocation density.

Numerous earlier studies on FSW of equivalent Al alloys were limited to examining the stirring zone's microstructure, microhardness, and bond strength. There are other reports on several Al alloys being friction stir welded.

FSW has several advantages from the beginning until the finish, including solid-state processing, direct routing, environmentally friendly, and energy efficiency. The main uses of FSW for microstructural modification in metallic materials include super plasticity, surface composites, uniformity of powder metallurgy aluminium alloys and AMMCs, three microstructural refinements of cast aluminium alloys, fatigue life improvement of arc welded joints, fabrication of metal foam and composites. The drawbacks of FSW for this project include holes, duty clamping arrangement, large downward forces, a lack of flexibility compared to arc welding, and equipment costs.

## **1.2 Working principle**

Thanks to the solid-state joining method, the two workpieces are joined without molten metal. During the FSW process, a tool not consumed when joining the workpiece is called a non-consumable tool. The sheet edges or plates that need to go in are inserted into one another, and a non-consumable rotating tool with a pin and a shoulder is pushed along the joining line until it reaches its conclusion. Due to the efficiency of its energy and environment safe nature, it is

the most crucial advancement in the metal joining process and is considered a "green" technology.

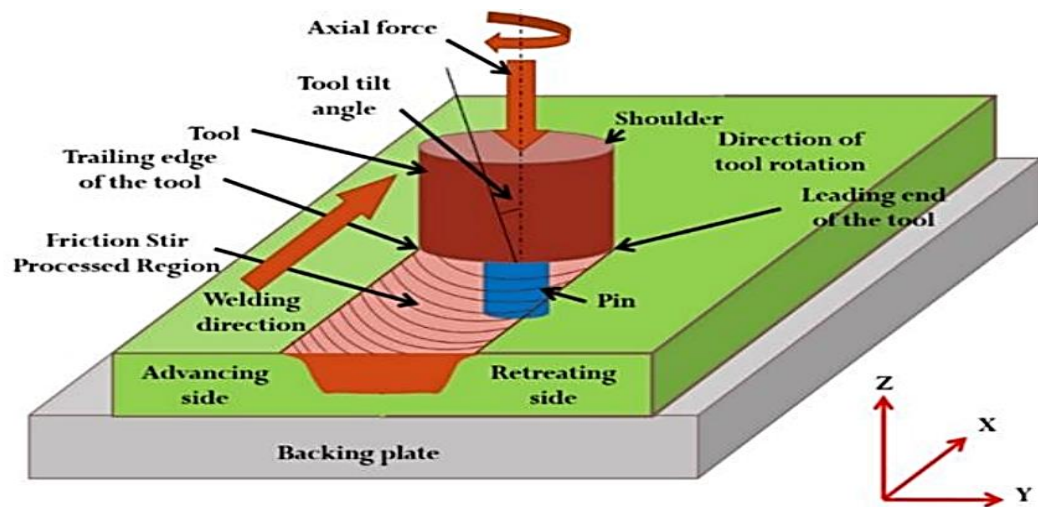


**Figure 1.1. Schematic illustration of friction stir welding**

Our work employs identical and different aluminium alloy metals and a few composite metals made of AA-6061 and AA-5083. Using an HSS tool and a taper pin with a circular cross-section, the joints are welded together utilising friction stir welding. To determine the two metals' respective strengths and harnesses.

### **1.3 RESEARCH OBJECTIVES AND APPROACH**

It is indispensable to comprehend the connection between microstructure joints and characteristics. The microstructure of a substance affects how hard it is. As a result, measuring hardness would be a suitable technique for examining irregular microstructures. Correlations between the microstructure, weld joint hardness, and for the sake of engineering materials development; a relation/link has been developed between Strength and Hardness.

### **1.4 FRAMEWORK OF THE THESIS**

The thesis is divided into chapters consisting of a literature review, results and discussion, and work reference in separate chapters.

### **1.5 FRICTION STIR WELDING**

Friction stir welding (FSW), a method of combining samples, was created by The Welding Institute (TWI). This approach alters the local microstructure of monolithic specimens to achieve particular and desired qualities by surface-changing the microstructure. A spinning cylindrical tool with a Shoulder and Probe (pin) is used in FSW to pierce a metallic plate before

moving along the surface of the workpiece. Frictional heat is produced when the shoulder of the tool rubs on the surface of the vessel. It softens the material beneath the shoulder, which is likewise severely deformed plastically by the revolving pin at a high strain rate. The material is exposed to metalworking techniques like friction, extrusion, and forging during FSW.

FSW has several advantages over traditional metalworking techniques, including being environmentally conscious, energy-saving, and a solid-state processing approach. The primary uses of FSW for microstructural modification in metallic materials involve superplasticity, surface composites, homogenisation of powder metallurgy aluminium alloys and AMMCs, microstructural refinement of cast alloys of aluminium, fatigue lifespan improvement of arc welded joints, production of metal foam and manufacturing of *ex-situ/in-situ* composites. Some downsides of FSW are the keyhole, heavy-duty clamping set up large downward forces, less flexibility compared to arc welding, and the expensive machine.

Friction stir welding (FSW), a solid-state welding method developed by The Welding Institute (TWI), UK, was first used to combine aluminium and its alloy [Thomas et al. [1], awes and Thomas, (1995)[1]]. Due to its energy economy, eco-friendly, and versatile nature, FSW has experienced the most remarkable development in metal joining during the last ten years and is considered a "green" technology. It can combine metallic alloys that are challenging to weld using traditional fusion welding processes, such as high-strength aerospace aluminium.

Based on the fundamentals of friction stir welding (FSW), friction stir welding (FSW) has been created. FSW is a brand-new thermo-mechanical processing method that may be applied to different microstructural alterations. The schematic depiction of friction stir welding is shown in Figure.1.1. The FSW's operation is very straightforward. An inert rotating cylindrical tool with a pin and shoulder that have been mainly created is utilised during FSW. High-speed rotation of the tool combined with a downward push causes the pin to pierce the material and contact the shoulder.

More heat is produced due to friction at the joint surface of the tool-workpiece, raising the temperature of materials to plasticity. The tool was then modified to move at the selected speed. The plasticised material flows around the pin as the tool advances, and the shoulder's forward motion helps to solidify it. The plasticised substance flows intricately around the tool as it moves from one side to the other. FSW is a thermomechanical technique in that material requires severe plastic deformation. In order to have a downward forging action of the tool, it



has been tilted by an angle of 1-3 degrees, and the plate shoulder of the tool consolidates the plasticised material concept. FSW can be applied locally to a specific component area without changing the qualities of the material overall because it does not alter the material's size or form. Since the material is deformed at high temperatures, this method can also handle alloys with limited ductility and HCP metals that are difficult to bend. Table 1.1 lists the key advantages of FSW while considering technical, metallurgical, energy, and environmental factors.

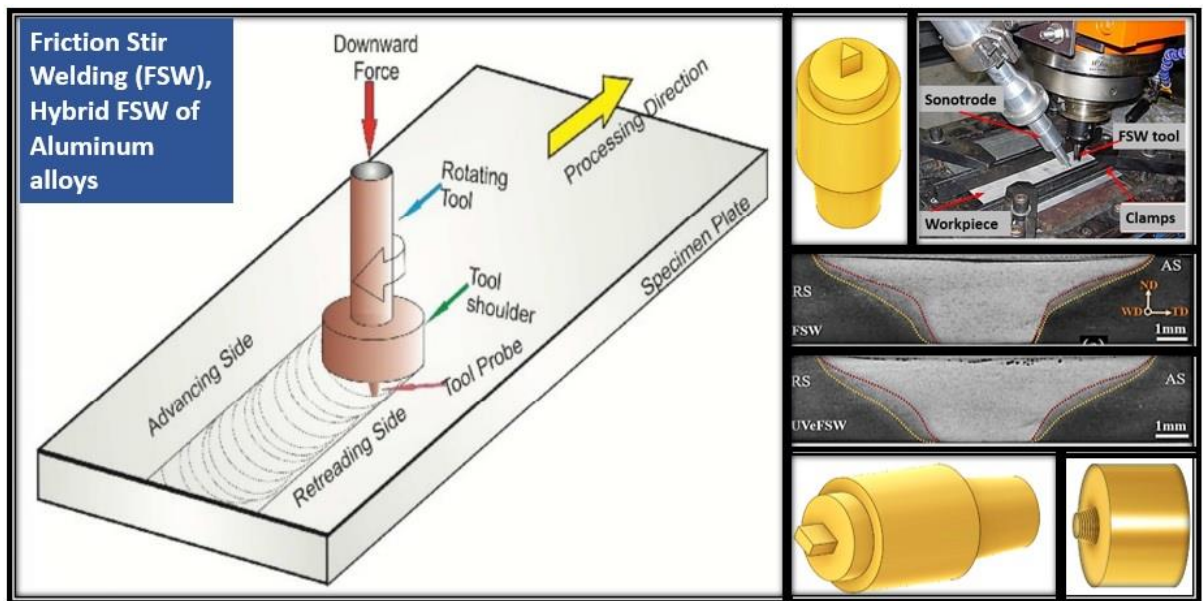


**Figure 1.2 Schematic process of FSW**

**Table.1.1 MAJOR BENEFITS OF FSW:**

Technical	<ul style="list-style-type: none"><li>• Technical features include a one-step process</li><li>• no surface cleaning is needed</li><li>• good dimensional stability</li><li>• good reproducibility</li><li>• processing depth regulated by pin length.</li></ul>
Metallurgical	<ul style="list-style-type: none"><li>• Metallurgical Solid-state processing</li><li>• Little part distortion</li><li>• Absence of chemical reactions Grain refining</li><li>• Excellent metallurgical properties</li><li>• No cracking</li><li>• Thermally sensitive material can be treated.</li></ul>
Energy	<ul style="list-style-type: none"><li>• Low energy consumption since the heat is generated by friction and plastic deformation.</li><li>• Energy-efficient compared to fusion-based systems like a laser because heat is produced by friction and plastic deformation rather than fusion.</li></ul>
Environmental	<ul style="list-style-type: none"><li>• There were no gases produced</li><li>• There was less noise.</li></ul>

### **1.6 Working of FSW**

1. Clamp both base metals after post-welding, i.e., cleaning, surface finishing, etc. Make no gap between base metals, and place them under the tool.
2. Next, until the tool shoulder meets the workpiece, a rotating tool pin is introduced into the workpieces at the surfaces of the base metal joining line. The material will be deformed plastically due to the friction's heating effect. Intermolecular diffusion will cause the material to bend plastically at this stage of the joining process due to heating from friction forces.
3. Along the joint line, the rotating tool is advanced. Behind the tool, a joint will result from this.

4. The tool keeps moving until the entire weld is produced. The tool is cut loose from the workpiece following the connecting procedure. The welding plates still have the tool pin's hole in them.

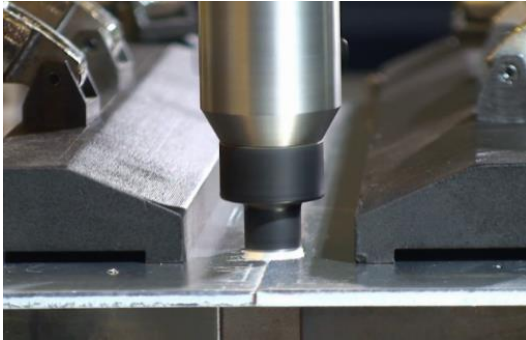


**Figure 1.2.1 FSW process in action**

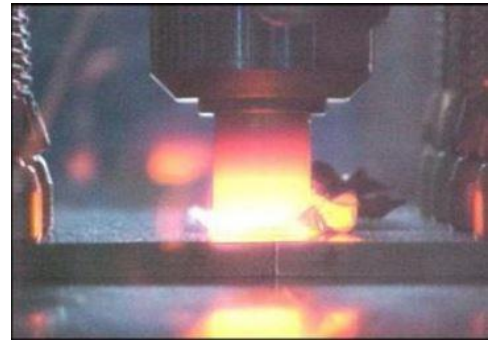


**Figure 1.2.2 Tool heated due to friction**

### **1.7 Aluminium (Al)**

One of the 13 elements listed on the periodic table, aluminium, is a silvery-white metal. Aluminium is the most prevalent metal on Earth and accounts for more than 8% of its core mass, which is a shocking fact about it. After oxygen and silicon, it is our planet's third most prevalent chemical element.

However, pure aluminium does not exist in nature since it readily combines with other elements. This explains why it was only recently that people heard about it. Although aluminium was first created informally in 1824, it took another fifty years for people to figure out how to manufacture it on an industrial scale.

Aluminium sulphates are the most prevalent type of aluminium in nature. These minerals combine two sulphuric acids, one based on an alkaline metal (lithium, sodium, potassium, rubidium, or caesium) and the other based on metal from the third group of the periodic table, mainly aluminium.

Aluminium sulphates are utilised in various fields, including cooking, cleaning water, medicine, cosmetics, the chemical industry, and other uses. By the way, the Latin word for aluminium, alumen, refers to the sulphates of aluminium.



**Figure 1.3 Aluminium metal element**

### **1.8 Application**

Depending on the application, aluminium can be used instead of other materials such as copper, steel, zinc, tin plate, stainless steel, titanium, wood, paper, concrete, and composites. The following sections provide some instances of the uses for aluminium.

#### **Packaging of aluminium**

Aluminium foils and sheets are frequently used in food packaging and protection due to their high resistance to corrosion, UV protection, moisture and odour confinement, and the fact that they are non-toxic and will not leach or taint the items.

the movement of aluminium

#### **Transport of aluminium**

The superior strength-to-weight ratio of aluminium has made it the go-to material for aircraft building since the beginning of the human-crewed flight. Due to the similar characteristics of aluminium, different alloys are currently utilised in motor vehicles, commercial vehicles, military vehicles, ships, boats, buses, coaches, passenger and freight rail carriages, commercial vehicles, and, increasingly, motor vehicles.

## **Marine Applications**

Increasing the size of a vessel above the waterline without causing stability problems is possible using aluminium plates and extrusions in the superstructure. Marine architects have achieved better performance with the available power due to aluminium's weight advantage by using aluminium in hovercraft, multihull catamarans, and surface planning vessels. Increasing the size of a ship above the waterline without causing stability problems is possible by using aluminium plates and extrusions in the superstructure. Marine architects have performed better using aluminium in hovercraft, multi-hulled catamarans, and surface planning vessels.

## **Foils**

Light, gases, oils and fats, volatile chemicals, and water vapour cannot pass through aluminium foil. Aluminium foil is employed in various applications due to its excellent formability, resilience to heat and cold, lack of toxicity, strength, and heat and light reflection. These applications include:

- Packaging and food safety
- Insulation
- Pharmaceutical packaging.

## **1.9 Need of aluminium (Al)**

When we analyse the seven designated aluminium alloy series for wrought alloys, we can quickly determine the primary alloying elements utilised to create each series. Analysis and research of these elements' impacts on aluminium are then possible. I have also added a few extra items that are frequently utilised. When we analyse the seven designated aluminium alloy series for wrought alloys, we can quickly determine the primary alloying elements used to create each series. Analysis and research of these elements' impacts on aluminium are then possible. I have also added a few extra items that are frequently utilised.

**Table 1.2 United States revised designation system for aluminium cast Alloys**

<b>code</b>	<b>Alloying element</b>
1xxx	Aluminium(pure)
2xxx	Cu
3xxx	Si with added Cu
4xxx	Si
5xxx	Mg
6xxx	Mg and Si
7xxx	Zn
8xxx	Ti

### **1.10 Aluminium used**

1. Aluminium alloys-6061
2. Aluminium alloys-5083

#### **1.10.1Aluminium alloys-6061**

A heat-treatable medium to high-strength aluminium alloy with a strength greater than 6005A is 6061. Despite having less strength in the weld zone, it is exceptionally corrosion-resistant and weldable. It is moderately resilient to tiredness in temper T4; it can be formed well in the cold but not as well in T6. For incredibly intricate cross-sections, unsuitable. The 6xxx series, a collection of alloys with silicon and magnesium as the main alloying elements, includes the 6061-aluminium alloy. Type 6061 aluminium has a nominal composition of 97.9% Al, 0.6% Si, 1.0% Mg, 0.2% Cr, and 0.28% Cu. Aluminium alloy 6061 has a density of 2.7 g/cm<sup>3</sup> (0.0975 lb/in<sup>3</sup>). The 6061 aluminium alloy may be heat treated, is simple to manufacture, is weldable, and has strong corrosion resistance.

### **Mechanical properties**

Young's modulus (E) : 68 GPa (9,900 ksi)

Elongation ( $\epsilon$ ) at break : 12–25%

Poisson's ratio ( $\nu$ ) : 0.33

### **1.10.2 Aluminium alloy -5083**

The 5083 aluminium alloy is renowned for its outstanding performance in harsh conditions. When exposed to industrial chemical conditions and seawater, 5083 is highly resistant to attack. After welding, alloy 5083 maintains its excellent strength. Although it possesses the maximum strength of non-heat-treatable alloys, it is not advised to use it above 65°C.

### **Mechanical properties**

Proof stress : 125Min MPa

Tensile strength : 275-350MPa

Hardness : 75HB

## **1.11 MICROSTRUCTURE DEVELOPMENT IN FSW**

Alteration of initial microstructures can be done in many ways using High Temperature and Strain Interaction. It results in three unique zones: the stir zone, the heat-affected zone (HAZ), and the thermomechanical-impacted zone (TMAZ). Each zone's strain rate, temperature, and different microstructural characteristics vary.

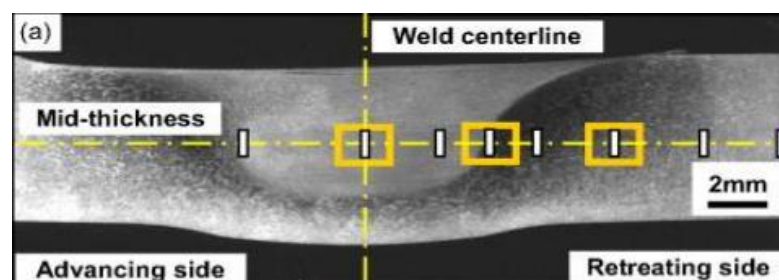


**Figure 1.4 (a) Macrostructure of the friction-stir welded 6061-T6 Al alloy.**

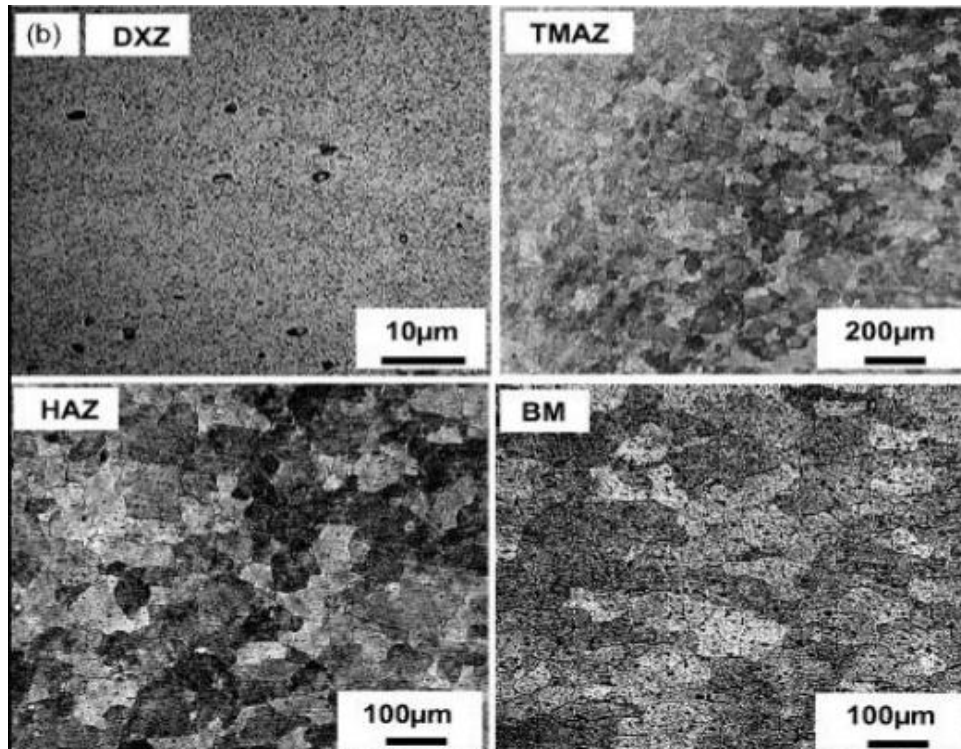


**Figure 1.4 (b) Microstructure of the dynamic recrystallised zone (DXZ), thermo-mechanically affected zone (TMAZ), heat-affected zone (HAZ), and initial base material (BM) taken at yellow square marks shown.**

**Stir zone:**

It is the area where temperature and deformation are at their highest. The stir zone, a nugget or dynamically recrystallised zone, is where the most grain refining occurs. Equalised, refined grains define the stir zone. The dimensions of the tool affect the stir zone's volume. Typically, the depth and width of the stir zone are determined by the pin length and shoulder width, respectively. Additionally, it has been reported that the grain size varies throughout the stir zone's volume. Variation can be found in the cross-section as well as the surface. The average grain size on FSW Al 6061 varies from 3.5 µm on the retreating side to 5.1 µm on the advancing side and from 3.2 µm at the bottom to 5.3 µm at the top. The gradients in strain, strain rate, and temperature the material endures during the intricate material flow are often to blame for this.

**Thermo-mechanically affected zone**

A thermomechanical affected zone (TMAZ) surrounds the stir zone's volume. The zone's dimensions range from a few micrometres to centimetres. The temperature in the TMAZ is lower than in the stir zone, and the strain rate is insufficient for dynamic recrystallisation. The zone is typified by grains with high dislocation densities that are elongated and distorted. In the



case of aluminium, achieving considerable plastic strain in this region without recrystallisation is possible. The recrystallised zone (weld nugget) and the deformed zones of the TMAZ typically have a clear separation.

### **Heat affected zone**

This region is in the middle of TMAZ and founding metal. The zone merely undergoes a heat cycle and no strain. Al alloys have a strong thermal conductivity, which causes some grain growth. In the Base Metal, the grains are less significant than in this zone. In some situations, the Retention of grain sizes of Base Metal is observed. For heat-treatable aluminium alloys, Mahoney defined a HAZ as the area exposed to temperatures more than 250°C.

### **Base material**

The material far away from the weld that has not been deformed and that, although it may have experienced a thermal cycle from the weld, is not changed by the heat in terms of microstructure or mechanical properties. According to Zahn Matkesh, the base material has huge, elongated pancake-shaped grains with an average size of 250 µm.

## **1.12 MATERIAL FLOW DURING FSW**

The tool shape, process parameters, and material properties play significant roles in FSW's highly complex material flow. However, according to several researchers, the material flow results from a combination of superficial shoulder-driven material churning and mixing and pin-driven extrusion. The probe shears the material from the 15 moving sides due to the tool rotating and moving linearly. It flows around the one pulling away, forging it under pressure in a mobile extrusion chamber enclosed by an excellent surrounding material and the tool.

According to Muthu Kumaran and Mukherjee, there are two forms of the metal transfer phenomenon are two kinds of the metal transfer phenomenon, according to Muthu Kumaran and Mukherjee. The first approach to the phenomenon of transfer of metal happens because of the movement of the shoulder. In contrast, the pin causes the combined effort of the shoulder, and the pin causes the second mode. The initially intended mode of metal transfer is impacted, and layers begin to stack up due to the material shifting from the advancing side to the retreating side each time the tool is rotated. Another method of transferring metal uses layer-by-layer material flow combined with material extrusion under plasticised conditions.

As the tool turns, the shoulder of the tool contacts the workpiece, generating heat, friction, and plastic deformation at the weld zone. Extrusion at the retreating forward and flanks might be occurring to The Metal.

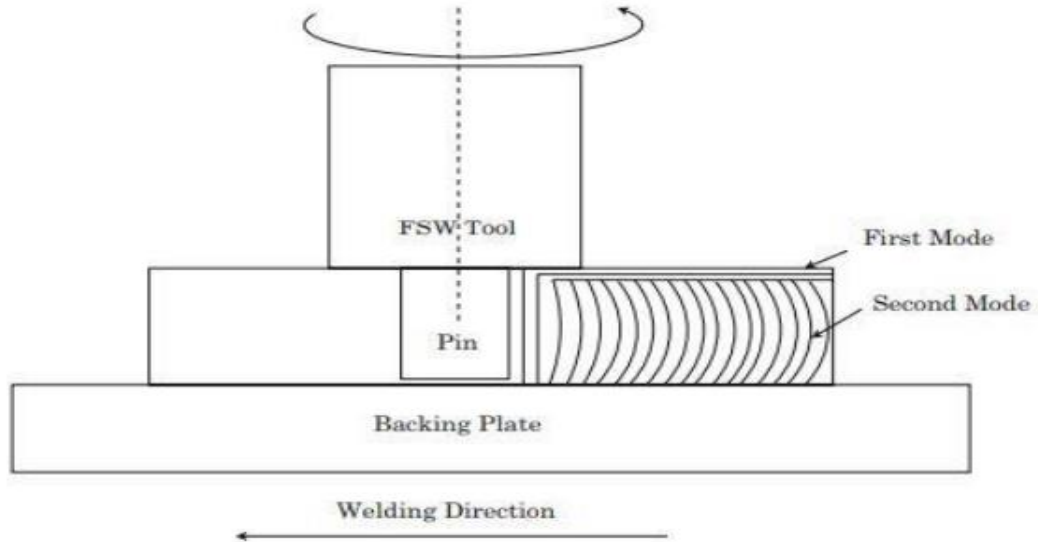


**Figure 1.5 Two Modes of Metal Transfer Phenomenon.**

The material is heated to a plastic deformation stage in the initial deformation zone. The shoulder bottom and pin influence the material flow. The stirring action of the pin causes the extrusion zone. The material is agitated from the side that is advancing to the side that is receding. The width of the extrusion zone changes according to the temperature distribution and stress concentration around the pin. After the forged zone, where the agitated material is made to set in a well-mixed state, the material from both sides of the final zone cools in the forging zone. Based on the cooling rate, the weld's tensile quality is affected.

FSW can be detected by looking at the microstructure of metal-to-metal welding. Steel spheres inserted at the weld centre line allowed Colligan to study the metal flow. The top surface of the weld is likewise said to experience chaotic mixing; however, no explanation is provided to support this claim. Reynolds investigated the metal flow of AA 2195-T8 in a number of friction stir welds using a marker insertion technique. According to a three-dimensional map from the deformed marker, there was no haphazard mixing of mixed material at the top layer.

When macrostructural analysis of the specimen is done perpendicular to the weld direction, concentric ring patterns are seen. According to reports, the structure resembles an onion ring pattern; as a result, the flow pattern's mechanism is called an "onion ring"; the onion rings are produced due to the interaction of two metal transfer modes. According to Schneider, Nunes,

and Krishnan, the geometry of onion rings is produced by a combination of shoulder compression and material extrusion at each tool pin revolution. According to Muthu Kumaran and Mukherjee, layer-by-layer material flow happens in the first and second metal transfer modes. The onion ring pattern is seen when the effects of the two metal transfer modes are combined.

### **1.13 Microstructure evolution during FSW**

Refined and equiaxed grains are produced in the stir zone as a result of the thermo-mechanical process known as friction stir welding (FSW). Dynamic recrystallisation (DRX) is widely regarded as the primary mechanism for grain refinement during FSW. However, other processes like recovery, recrystallisation, precipitating, breakdown, and local weakening may also occur. It has been proposed that a variety of dynamic recrystallisation processes, such as dynamic recovery (DRV), geometric dynamic recrystallisation (GDRX), discontinuous dynamic recrystallisation (CDRX), and continuous dynamic recrystallisation (CDRX), can help refine the grain during FSW of various alloys.

High stacking fault energies in aluminium and its alloys result in speedy dynamic recovery (DRV) during FSW, which prevents the build-up of stored energy by displacement concentration within the substance. Dislocations are encouraged to climb and cross slip, which are the main processes for recovery, by high piling fault strength. In the stir zone of the welded material, DRV rearranges dislocations to produce sub-grains with practically dislocation-free interiors, which helps to create delicate and equalised grains.

During DRV, the Zener-Holloman parameter, which is given by, expresses flow stress, strain rate, and temperature.

$$Z = \dot{\epsilon} \exp (Q/RT)$$

For a particular temperature and strain rate, Z determines the sub-grain size; while for lattice diffusion, Q determines the activation energy.

When the formula and a critical distortion condition are often applied to hot working operations where the strain rate and temperature are well-known, DDRX occurs.

It has been attained and calls for extensive high-angle border migration. A condition for initiation of DDRX is given by

$$\frac{\rho_m^3}{\dot{\epsilon}} > \frac{2\gamma b}{KLMGb^5}$$

Where;

M is Boundary Mobility,

G is Shear Modulus,

B is Burgers Vector, and

$\rho_m$  is Mobile Dislocation Density.

K is a Constant percentage of the Dislocation Line Energy stored in the Newly Formed Grains.

L is the Mean slip distance of the dislodgments in these grains.

The likelihood of DDRX is decreased by the high recovery rate, which happens in materials with more fault-energy stacking and lowers  $m$ , specifically at high strain rates. A crucial deformation originating at high-angled borders is required to start dynamic recrystallisation. 20 Due to their rapid recovery rate and the high stacking-fault energy of Al, aluminium and its alloys often do not experience DDRX.

In comparison to DDRX or CDRX, geometric dynamic recrystallisation (GDRX) differs in that the initial grains flatten, i.e., compression or lengthens (tension, torsion), and their borders become with time notched as sub-grains develop. The grain borders eventually come into contact locally, pinching off the grains and generating newly remote grains when the Grain Thickness is decreased to about two Sub-Grain Sizes [McQueen et al., 1991]. When previous boundary separation reaches sub-grain size related to  $Z-1$ , during DRV, GDRX may be seen.

$$d_n = d_0 \exp(-\epsilon)$$

Where;

Initial grain size is denoted by  $d_0$ , while a strain is denoted by  $\epsilon$ . Low strain rates and stressors cause the tiny  $Z$  value and the initial start of GDRX. Higher Strain Rates will result in a more extended DRV stage of deformation before the commencement of GDRX.

Friction When grain boundaries are stir-welded (FSW), geometric dynamic recrystallisation (GDRX) is induced, whereby the serrated grain borders pinch off to produce freshly, refined

particles when the grooved borders cross. The foundation for comprehending the mechanics of grain refinement under FSW is provided by the microstructure seen in the stir zone. The evolution of refined grains has been studied using a tool plunge and extraction technique, followed by annealing, to simulate FSW conditions. The mechanisms for grain refining during FSW of 7050 Al have been identified as nucleation (DDRX) and growth. Recent studies have been devoted to understanding how FSW in aluminium and related alloys heals, revealing grains with different dislocation densities and degrees of recovery. It has been proposed that many mechanisms, including DDRX, DRV, and CDRX, act at various stages of microstructure generation due to heterogeneous plastic deformation. Fine granules between 100 and 400 nm have been linked to the development of discontinuous DRX.

#### **1.14 Material used for the tool**

##### **HIGH-SPEED STEEL**

Because they can cut materials more quickly than the conventional high-carbon steel traditionally used as cutting tools, high-speed tool steel alloys were created. Due to the alloying metals and heat treatment utilised, it possesses unusually high hardness, abrasion resistance, and resistance to softening at high temperatures. According to the American Society for Testing & Materials' Specification A600-79, high-speed steel is high-carbon steel containing tungsten, molybdenum, chromium, vanadium, and occasionally cobalt.

Even though "high-speed tool steel" refers to a variety of alloys, they all share these characteristics:

- Molybdenum or tungsten make up most alloys, with only trace amounts of chromium, vanadium, or cobalt
- high carbon content, typically between 0.8% and 1.5% by weight, with a minimum Rockwell hardness of 64 HRC at room temperature
- Hardness and wear resistance are produced via an alloying process, resulting in a high concentration of complex metallic carbides, primarily tungsten, molybdenum, and vanadium carbides, suspended in a steel substrate.



**Figure 1.6 Friction stir welding on similar Aluminium alloys**

#### **1.14.1 Tool materials**

Thermo-mechanical deformation, known as friction stirring, occurs when the tool temperature reaches that of the workpiece's solidus temperature. The Selection of Proper Tool Material for the intended application is necessary to produce a high-quality friction stir process. All friction stir tools have features intended to serve a particular purpose.

#### **Tool Material Selection**

Tool materials utilised in friction stir welding include tool steels, nickel- and cobalt-base alloys, refractory metals, carbides and metal-matrix composites, and cubic boron nitride. The tools primarily utilised for welding high-strength materials include refractory materials like tungsten alloys and Poly Crystalline Boron Nitride (PCBN). However, connecting and treating aluminium alloys and their composites substantially use tool steel.

## **Tool Material Characteristics**

Numerous different material properties could be ranked as necessary for friction stir welding, depending on factors like the material of the workpiece and the projected tool life. The choice of tool material may be influenced by more than just a material's physical characteristics.

### ➤ **Strength at Ambient and Raised Temperature**

To avoid tool breakage or falsification during the friction stir weld, the tool material must sustain compressive stresses when the tool hits the workpiece and possess enough oppressiveness and shear strength at high temperatures.

### ➤ **The stability of elevated temperatures**

Maintenance of strength and dimensional stability of the Tool while using enough strength at high temperatures.

### ➤ **Wear Resistance**

The tool's shape is altered by excessive tool wear, which limits the weld quality and raises the possibility of flaws. Tool wear can happen during friction stir welding by 24 different adhesive, abrasive, or chemical causes. The communication in middle of the workpiece and tool materials and chosen parameters determines the precise wear mechanism.

### ➤ **Fracture Toughness**

Even with mitigating techniques (a pilot hole, a modest plunge speed, and workpiece preheating), the initial resident stresses and strains created when the tool contacts the workpiece are enough to shatter the tool. It is widely acknowledged that the tool dive and abide stages cause the maximum outstanding amount of tool damage.

### ➤ **Tool Reactivity**

Materials for tools must not react with the workpiece or the environment because this would alter the tool's surface qualities.

## **1.15 Defects in FSW**

Improper selection of processing conditions results in stirred / weld zone defects. Similar kind defects were observed in both processes. Table 1.3 shows common types of defects observed in FSW. Defects include wormhole, scalloping, ribbon flash, cavity, surface lack of fill, nugget collapse and surface.

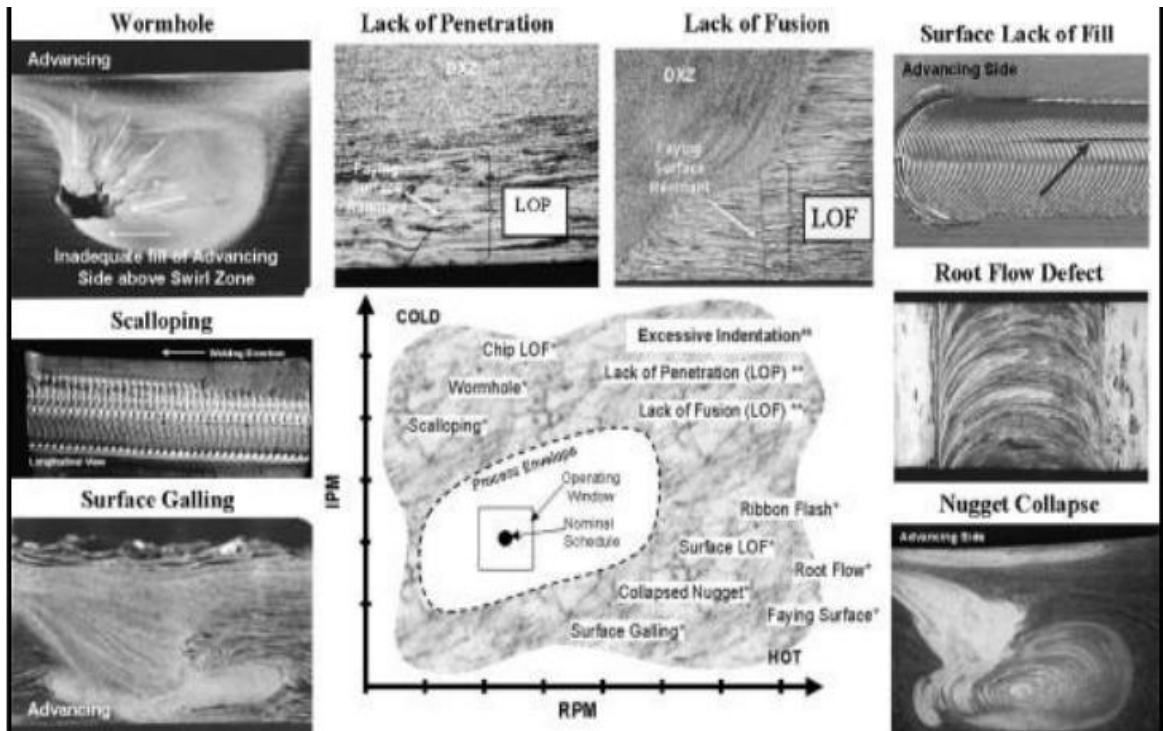


**Figure 1.7 Characteristics of flaw types in friction stir welding**

#### 1.16 Application of Friction Stir Welding:

1. FSW is used in aircraft industries for welding wings, fuel tanks, aircraft structures, etc.
2. Used in marine industries for structure and framework.
3. Used in automobile industries to weld wheel rims, chassis, fuel tanks, and other structural work.
4. Chemical industries use it to join pipelines, heat exchangers, air conditioners, etc.
5. Friction stir welding is also used in electronic industries for joining bus bars, aluminium to copper, connectors, and other electronic equipment.



**Table 1.3 Common types of defects observed in FSW**

<b>S.no</b>	<b>Defects</b>	<b>Probable reason</b>
<b>1</b>	<b>Wormhole</b>	Usually found on the advancing side <ul style="list-style-type: none"> <li>• Insufficient forging pressure</li> <li>• Too high of welding speed</li> <li>• Insufficient workpiece clamping</li> </ul>
<b>2</b>	<b>Lack of penetration</b>	Geometric flaw <ul style="list-style-type: none"> <li>• Improper placement of the tool</li> <li>• Workpiece gap, thickness mismatch or plate thickness variation</li> <li>• Incorrect tool pin length, too high of welding speed,</li> </ul>
<b>3</b>	<b>Excessive flash</b>	<ul style="list-style-type: none"> <li>• Material expulsion in the form of excessive surface flash formation.</li> <li>• Too high welding speed,</li> <li>• High forging load.</li> </ul>
<b>4</b>	<b>Nugget collapse</b>	<ul style="list-style-type: none"> <li>• Inadequate nugget shape creation towards the retreating side</li> <li>• Excessive flow arm formation and material injection into the advancing side</li> <li>• Overly hot weld</li> <li>• Insufficient weld pitch</li> </ul>
<b>5</b>	<b>Surface lack of fill</b>	<ul style="list-style-type: none"> <li>• On the side that is moving forward, a constant top surface void</li> <li>• Insufficient top surface flow arm formation</li> <li>• Insufficient plunge depth</li> <li>• Insufficient forge pressure</li> </ul>
<b>6</b>	<b>scalloping</b>	<ul style="list-style-type: none"> <li>• Sticking of metal to pin tool.</li> <li>• Excessively hot weld,</li> <li>• Too high weld pitch</li> </ul>

## CHAPTER 02

### LITERATURE REVIEW

#### FSW Process Analysis

- **Thomas et al. [1]** The Welding Institute (TWI) examined the issue of utilising aluminium alloy fusion welding. Using friction stir welding (FSW) prevents base material surface oxide development. FSW employs a non-consumable tool to join metal that generates heat due to friction between the base material and the tool.
- **Lohwasser et al. [2]** asserted that pin-driven and shoulder-driven material flows are feasible in FSW. The creation of an oxide layer impacts the strong bonding of the material. Using the tool shoulder in FSW prevents the production of this oxide layer. Working temperatures for FSW are roughly 0.6 to 0.9 times melting temperatures.
- **Cavaliere et al. [3]** examined the tensile and fatigue properties of FSW 2024 and 7075 alloys. The tensile test revealed that 2024 failed due to lesser hardness, and 7075 failed due to shorter fatigue life.
- **Sundaram et al. [4]** used five different pin profiles to analyse the friction stir welding for AA2024-T6 and AA5083-H321. When comparing the cylinder with a taper tool pin diameter to the triangular pin, flat cylindrical pin, and cylindrical threaded profile, the cylinder with a taper tool pin diameter is the key factor causing the higher tensile strength. Additionally, they discovered that a defect-free weld might be produced at axial forces of 4 to 8 kN, 15 to 35 mm/min, and 300 to 700 rpm.
- **Leitao et al. [5]** Researchers compared the mechanical behaviour of two different alloys, AA5182-H111 and AA60616-T4, and discovered that for AA5182-H111, the grain size had a significant influence on the joints' tensile strength. It examined A319 and A413 and found that the welded joint had lost some flexibility.

#### Aluminium Alloy 5083

- **El-Rayes et al. [6]** examined how feed rate affected the mechanical and microstructural characteristics of friction stir welded joints with AA5754. They observed that grain sizes were smaller and grain boundaries were greater at increased feed rates. It improved the yield and tensile strength of the welded joints, with decreased ductility.
- **El-Sayed et al. [7]** examined how FSW factors affected the peak temperature and mechanical characteristics of welded joints made from AA5083-O. They concluded that the

welding peak temperature is not significantly affected by changes in either transverse speed or tool pin profile. Additionally, they discovered that using a threaded tool pin at welding speeds of 50, 100, and 160 mm/min resulted in flawless welds with higher tensile strength values.

- **PALANIVEL et al. [8]** studied how different aluminium alloys (AA6351 and AA5083-H111) welded using traditional FSW differed in their mechanical and metallurgical properties. Although traditional FSW is frequently used for welding materials that are different from one another, it is difficult and time-consuming.
- **MOFID et al. [9]** compared Al5083 and AZ31COMg joining of different materials to UFSW and FSW. The results demonstrated that FSW lowered the incidence of the intermetallic phase and increased the number of refined grains in the welds. However, the joints hardened because the stress zones experienced optimal peak temperatures.
- **MOFID et al. [10]**. Examined whether connecting various aluminium/magnesium alloys (AA5083-H4 and AZ31) using UFSW and SFSW in cryogen was feasible. They concluded that SFSW suppresses the synthesis of the interatomic molecule at low peak temperatures.
- **SUNDARAM and MURUGAN [11]** examined how the pin profile used in FSW affected the mechanical qualities of two different aluminium alloys, 2024-T6 and 5083-H321, where the alloy with the higher strength (2024) was placed on the retreating side (RS). The research demonstrated that a plastic flow of material, reduced tensile strength, and reduced elongation are exhibited when the combinations of factors produce extremely low or extremely high frictional heat.
- **Peel et al. [12,13]** reported the residual stress and so-called processing window of the different FSW 5083- Al6082Al alloys.
- **Miles et al. [14]** focused on the formability of FSW joints made from different aluminium alloys in the 5xxx to 6xxx series that may be used to create 'custom blanks' following technical specifications. Due to its excellent design efficiency and affordable processing, FSW of different aluminium castings to wrought plates has so far found growing use in the fabrication of aviation and missile components.
- **Mohammad Hasan Shojaeefard et al. [15]** studied the mechanical characteristics of the welded AA7075-O and AA5083-O alloys. An ANN model was created to forecast the UTS and hardness of aluminium as functions of welding and rotational speeds. The ANN model produced excellent results.

## Aluminium Alloy 6061

- **Shah et al. [16]** performed FSW on AA6061 to evaluate how tool eccentricity affects the material flow and the welded connections' mechanical characteristics. Their results showed that tool offset produced better material flow than the conventional one, which increased the stir zone's (SZ) temperate region. However, the tool offset the natural mechanical characteristics of the welded joints.
- **Abdulstaar et al. [17]** studied the mechanical characteristics of the shot-peened welded joints and the microstructure over the thickness of the AA6061-T6 friction stir weld joints. According to the specimens evaluated using electron back-scattered diffraction (EBSD), the coarsest grains, measuring 5  $\mu$ m, were found at the top of the welded joint. In contrast, the finest ones, measuring 2  $\mu$ m, were found at the root. Additionally, the welded joints' fatigue strength was lower than the BM's. The Almen intensity of the shot-peened ones increased from 0.18 to 0.24 mmA, whilst the shot-peened ones had superior fatigue properties.
- **Yuvaraj K.P et al. [18]** The Taguchi Technique performed FSW on the AA7075-T651 and AA6061 aluminium alloys. The results of the FSW demonstrated that tool-related parameters, such as the offset value of the tool, tool pin profile/shape, and tilt-angle  $\alpha$ , had a significant impact on the outcomes. It is now understood that the Taguchi technique's optimisation of the process parameters allowed for creating different FSWs.
- **SADEESH et al. [19]** AA6061 and AA2024 alloys were friction stir welded using a variety of pin shapes. The findings indicated that, compared to the strength attained when tapered and cylindrical pin profile tools were employed, the tensile strength of the joints conducted with the squared-pin profile tool improved.
- **MAHTO et al. [20]** evaluated the viability of continuous fillet stir welding (CFSW) and UFSW for joining sheets of two different materials (AA6061-T6 and AISI304). Figures 18 and 19 investigated how welding tool rotational speeds and plunging depth (PD) affected the strength and weld quality of the junction. The synthesis of thick intermetallic compounds was prevented by less heat.
- **Li et al. [21,22]** gave clear pictures of complex flow patterns and visualisation in different FSW alloys 2024Al to 6061Al. To restore the mechanical characteristics of the dissimilar FSW of 7075Al-O to 6061Al-O alloys, post-weld heat treatment (PWHT) was applied.

- **Rathinasuriyan et al. [23]** have created a mathematical model to optimise the SFSW parameters for the aluminium alloy 6061-T6's maximum tensile strength. Through underwater FSW, they achieved an ultimate tensile strength of 211.46 MPa.
- **Rajkumar et al. [24]** created an empirical model using linear regression to estimate the tensile strength and grain size for FSW of AA6061-T6 alloy.

### **Aluminium Alloy Composites**

- **Prabhu et al. [25]** created FSW joints from AA6061-3% rutile composite and mechanically and microscopically analysed the joints. They concluded that rotational and welding speeds significantly impacted the junction's mechanical and material features. Due to the increased stirring action of the tool and the mutual interaction of the rutile particles on each other, the microstructure of SZ was made up of recrystallised, uniformly dispersed, finer equiaxed grains with numerous microscopic rutile particles. Furthermore, due to faster dynamic recrystallisation and improved mechanical characteristics, the square tool pin profile created finer grains in the SZ than the cylindrical threaded one. With a maximum joint effectiveness of 97% at 100 rpm and 90mm/min, the grains at the bottom of the SZ were also finer than those at the top.
- **Kalaiselvan et al. [26]** discussed characterising the stir-cast composite material made from AA6061 and B4C. The distribution of boron carbide (B4C) particles and elongated grains in the TMAZ could be seen as parallel bands in the microstructure evolution data. In contrast, the SZ showed the homogenous distribution of these particles and some degree of fracturing. While the tensile strength under the testing conditions was comparable to the parent composite's strength, the weld zone hardness recorded a higher value than the BM. However, after the FSW procedure, it demonstrated a decline in the ductility of the joint and a change in the fracture mode from ductile to brittle.

### **Cahoon Equation**

- **Njuke et al. [27]** discovered an empirical relationship between the tensile strength of medium carbon steel quenched in various cooling regimes and Rockwell hardness. They reported that it is possible to forecast the tensile strength of quenched steel by using measured hardness values.

- **Zhang 23 et al. [28]** tried to establish a correlation between the hardness and strength of three materials: bulk metallic glasses with brittle grains, ultrafine-grained materials, and coarse-grained materials. They concluded that the correlation between hardness and strength depends on dislocation pile-up and its shear deformation.
- **Pavlina et al. [29]** We collected considerable data on various microstructures and compositions of austenitic hypo-eutectoid steels. Regression analysis was used to build a linear relationship between hardness and hardness strength using multiple data.
- **Lu et al. [30]** We also created an empirical relationship between the tensile strength and hardness of a laser-welded Ti-6Al-4W joint. Based on the observations of hardness, they claimed that the linear relations might be used to forecast strength in narrow welded and heat-affected zones.
- **CAVALIERE et al. [31]** said that thorough investigation and qualification work in this area is necessary. Despite the significant use of FSW as a commercial joining technique, the connection between the joint's microstructure and characteristics is poorly understood.
- **GAŠKO and ROSENBERG [32]** described the relationship between tensile characteristics and hardness in dual-phase steels of extremely high strength.
- **SHEN [33]** researched the relationship between tensile strength and hardness in particle-reinforced metal matrix composites.

## 2.2 Objectives

1. To execute friction stir welding to combine two identical aluminium alloys.
2. To execute friction stir welding to combine two different aluminium alloys.
3. To make sure that, while welding, the proper weld joint forms.
4. To research the two weld junctions' mechanical characteristics.
5. To investigate the tensile strength at weld joints that are welded under various circumstances.
6. To investigate the hardness characteristics of the weld joints when friction stir welding is carried out under various circumstances.
7. To study the yield strength at the weld joint.
8. To collect data on UTS, YS, and HV of various similar FSW joints.
9. To collect data on UTS, YS, and HV of various dissimilar FSW joints.
10. To collect data on UTS, YS, and HV of various composite reinforced FSW joints.

11. To plot graphs to understand the relationship between TS and HV using OriginPro software.
12. To analyse the relationship between hardness and strength of various data collection and experimental data during friction stir welding.

## CHAPTER 3 MATERIALS AND METHODOLOGY

### 3.1 Materials

1. Aluminium A6061
2. Aluminium A5083
3. Composites

### 3.2 Friction Stir Welding

In this investigation, the elemental composition of the basic materials—AA5083-H111 and AA6061-T6 aluminium alloys—was determined by butt-joining them along the rolling direction with an FSW machine (Make: RV Machine tools, Coimbatore, India, Model: FSW-3T-NC). The FSW experiment, FSW tool dimensions, tensile sample dimension, and Notch tensile sample dimensions are schematically depicted in Figure. 3a–b. With a pin diameter of 6mm at the root and 4mm at the pin tip, a pin length of 5.5mm, and a shoulder diameter of 18mm with 30 concavity, a conical tapered threaded pin profile made of H13 tool steel was employed. The studies used a constant tool tilt angle of 10 and plunge depth of 0.2mm. AA5083 and AA6061 were positioned on the advancing side (AS) and retreating side (RS), respectively, and FSW joints were created utilising six distinct welding parameter combinations (tool traverse and rotating speed).

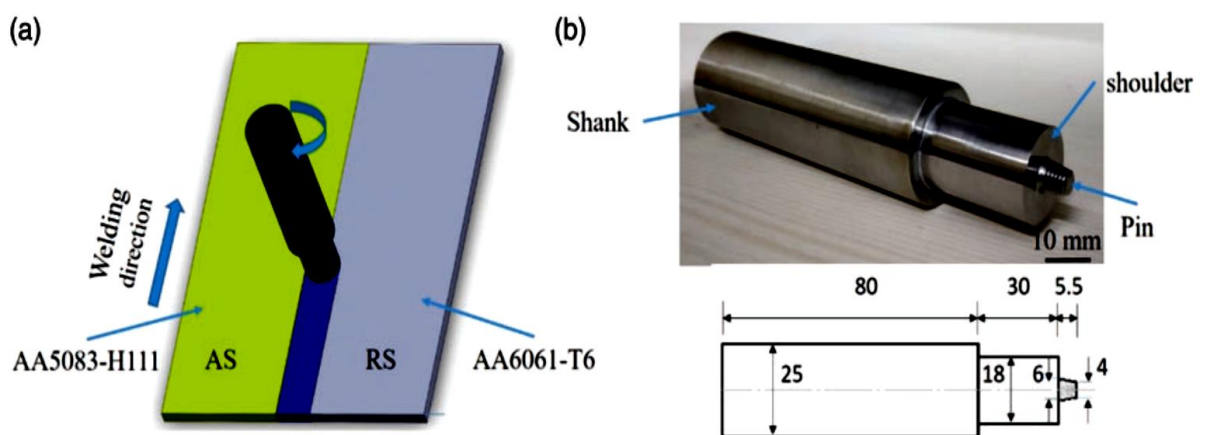


**Figure 3.1(a) FSW schematic illustration**

**(b) FSW tool with dimensions**



The joints were initially created using FSW at various traverse speeds of 40, 60, and 80 mm/min while maintaining a constant rotational speed of 800 rpm. Later, joints were created while maintaining a constant traverse speed of 60 mm/min at the various rotating speeds of 1100, 1400, and 1700 rpm. According to the chosen procedure parameters, the samples were given names. For instance, 800-40 denotes a sample with a rotational speed of 800 rpm and a traverse speed of 40 mm/min.

### **3.2.1 FSW Machine**

Friction stir welding (FSW) is a solid-state joining technique that joins two facing workpieces without melting the material of the workpieces. Heat is produced due to friction between the revolving tool and the material of the workpiece, which causes a softened area close to the FSW tool. The two pieces of metal are mechanically mixed as the tool moves along the connection line, much like how clay or dough is joined, and the tool's application of mechanical pressure forges the hot, softened metal. It is often applied to wrought or extruded aluminium, especially for buildings requiring solid welds. Mild steel, stainless steel, titanium alloys, magnesium alloys, and aluminium alloys can all be joined using FSW. It was successfully utilised to fuse polymers more recently. FSW has lately succeeded in connecting incompatible metals, such as aluminium and magnesium alloys. FSW is used in contemporary shipbuilding, rail transportation, and aerospace applications. It was successfully utilised to fuse polymers more recently. FSW has lately succeeded in connecting incompatible metals, such as aluminium and magnesium alloys. FSW is used in contemporary shipbuilding, rail transportation, and aerospace applications.



**Figure 4.2 FRICTION STIR WELDING MACHINE**

A four-axis CNC-controlled friction stir welding equipment created by BISS-ITW, Bengaluru, India, performed a friction stir welding process. Figure.3.2 depicts the FSW apparatus used in this investigation. Table 3.3 displays the specifications of the device. Friction stir processing is described in Figure.3.3a. During FSP, a significant amount of axial and transverse force is produced, which results in the workpiece's thermal expansion and buckling. In all of the experiments, the stiff fixture with bolted systems was employed to prevent this deformation of the workpiece plates, as illustrated in Figure.3.1.

### 3.2.2 Mechanical Testing

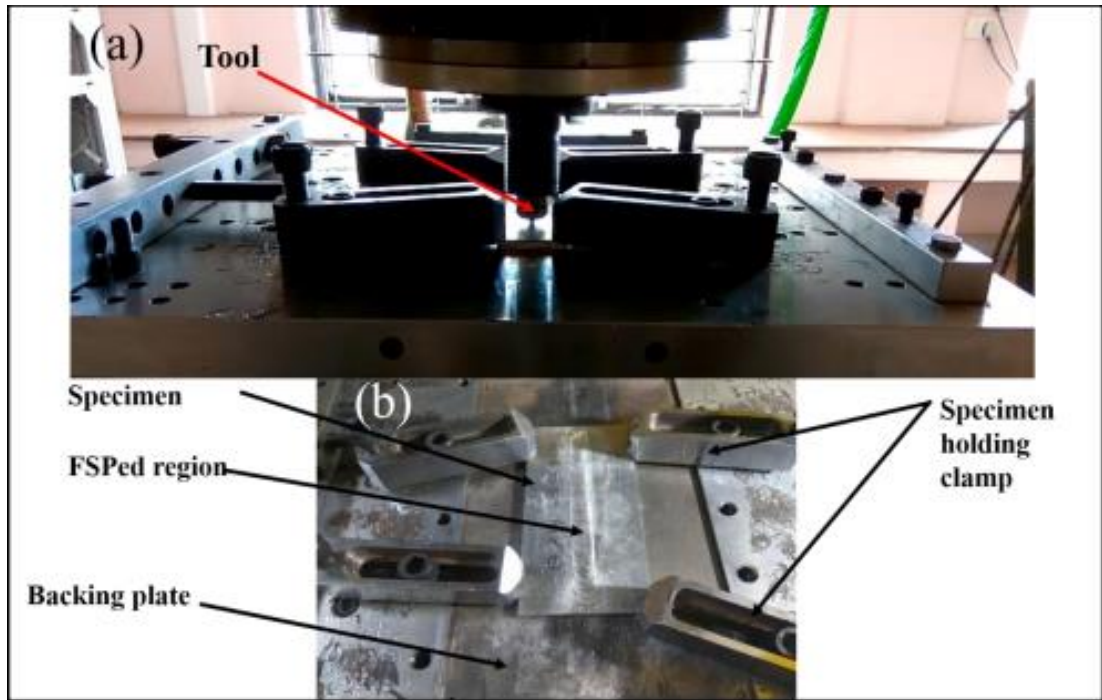
The hardness of different welded specimens was measured at the midpoint and along the transverse cross-section using a Vickers microhardness tester (Make: Chennai Metco, Model: Economet VH-1). At 0.5mm intervals, the hardness testing was conducted with a 0.1-kilogramme weight. The ASTM E8M-04 standard made the transverse tensile and notch tensile samples, and Figures 5(c) and (d) depict a schematic diagram of the specifications. The tests were conducted at room temperature using a universal testing machine (UT) with a 100kN capacity and a crosshead speed of 0.5 mm/min (Make: Fine Spray India, Model: M-100). To examine the notch tensile strength behaviour of FSWed joints, the notch tensile test was conducted for failure to occur at the SZ. Three samples were constructed for the transverse and notch tensile tests for each welding condition.



Figure 3.3 Control system

**Table 3.1 Specification of 4-axis friction stir welding**

Z AXIS	Load Stroke length Rate of movement Accuracy	50 KN 300 mm 1-100 mm/min + or – 6 microns
X-Y AXIS	Load Stroke length Rate of movement Accuracy	50 KN 500 mm 5-3000 mm/min + or – 6 microns
X&Y AXIS SERVO MOTORS	Speed Torque Power	2000 rpm 37 Nm 7.75 KW
X&Y AXIS GEAR MOTORS	Ratio Backlash	3 6 Arcmin
SPINDLE SERVO MOTORS	Spindle speed Spindle torque Power	3000 rpm 100 Nm 30 KW
Tool tilt in the Y axis	-	+ or - 5°
Power pack	-	4 LMP
Control system	-	UACE 2020



**Figure 3.3 (a) Friction Stir Processing with a Tool, (b) Fixture Setup.**

### 3.2.3 Tool used for FSW



**Figure 3.4 FSW process on dissimilar Aluminium alloys**

### 3.2.4 Tool parameter

Tool Material : High-Speed Steel

Feed Rate : 30mm/sec

Rotation Speed : 1000 RPM

### 3.3 Hardness Test

A material's hardness is a quality, not a fundamental physical trait. Its definition is "resistance to indentation," Its measurement is the indentation's permanent depth.

The Rockwell scale measures a material's resistance to indentation as a measure of hardness. The Rockwell test examines an indenter's penetration depth under a considerable load (significant load) compared to the penetration made by a preload (small load). Different scales employ various loads or indenters, each identified by a single letter. A result is a dimensionless number with the suffixes HRA, HRB, HRC, etc., where the last letter stands for the appropriate Rockwell scale.

The hardness profile was carried out on a transverse segment parallel to the FSW direction.

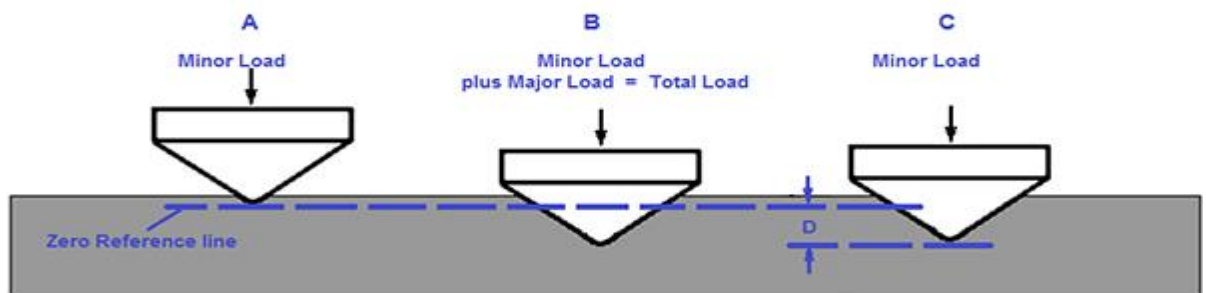
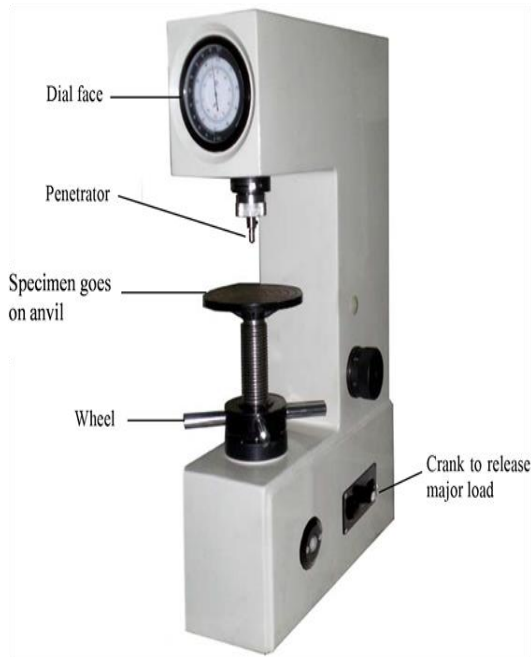


Figure 3.5 Hardness Test Process



**Figure 3.6 Hardness testing machine**



**Figure 3.7 B- Scale indicator**

### 3.4 Tensile Test

A Tinius Olsen tensile testing equipment with a starting strain rate of 1 mm/min was used for the tensile tests. The samples were made per ASTM E8/E8 M-49 11 standards and had the following dimensions: 4 mm thick, 6 mm wide, 20 mm gauge length, 12 mm grip section width, 12.5 mm fillet radius, and 60 mm overall length.

UTMs, often referred to as materials testing machines or materials test frames, are used to assess materials' tensile strength and compressive strength. Tensometers were the original name for tensile testing equipment.



**Figure 3.8 Universal Testing Machine(UTM)**

### **3.4.1 Specifications of Tensile Testing Machine**

Type : Universal Testing Machine (UTM)

Make : FIE

Model : UTE-20

Capacity : 20 Tons

Oil Pump Output : 1.5 lit/min

Motor for Oil Pump : 1 H.P

Motor for Cross Head : 0.33 H.P

## CHAPTER 4: RESULTS AND DISCUSSION

### 4.1 Friction stir welding:

### 4.2 Correlation between strength and microhardness:

Any point's ultimate tensile strength and yield strength might be calculated using the proper relationships between hardness and these strengths. The generated data can subsequently be shown as distribution maps to see intensity fluctuations quickly. CAHOON et al. [34,35] provided two equations that used the strain hardening coefficient, which was based on total strain rather than real plastic strain, to relate the hardness of materials to their yield and tensile strengths:

$$\frac{\sigma_Y}{HV} = \frac{(0.1)^n}{3} \quad (1)$$

$$\frac{\sigma_{UTS}}{HV} = \frac{1}{2.9} \left[ \frac{n}{0.217} \right]^2 \quad (2)$$

where n is the strain hardening coefficient, Y is the yield strength, and UTS is the ultimate tensile strength in MPa 10<sup>-1</sup>. where HV is the Vickers hardness.

According to CAHOON et al. [34,35], the H/3 coefficient is appropriate for calculating Y for aluminium; however, some assumptions must be considered to update the H/2.9 coefficient for aluminium in calculating UTS. According to CAHOON, the value of actual stress at the apex of the stress-strain diagram is H/2.9 [34,35]. Their engineering quantities can be used to determine the real stress and strain.



### 4.3 Experimental results

#### 4.3.1 Results obtained from Dissimilar AA6061 – AA5083 FSW weld(case 1)

Table 4.1 UTS, YS, and HV values obtained from AA6061- AA5083 FSW welded joints

	YS [MPa]	UTS[MPa]	Hardness[HV]
AA5083	180	310	85
AA6061	221	295	79
700-30	156	251	69
700-50	159	242	72
700-70	172	231	76
900-50	187	298	77
1100-50	192	241	68
1300-50	149	234	57

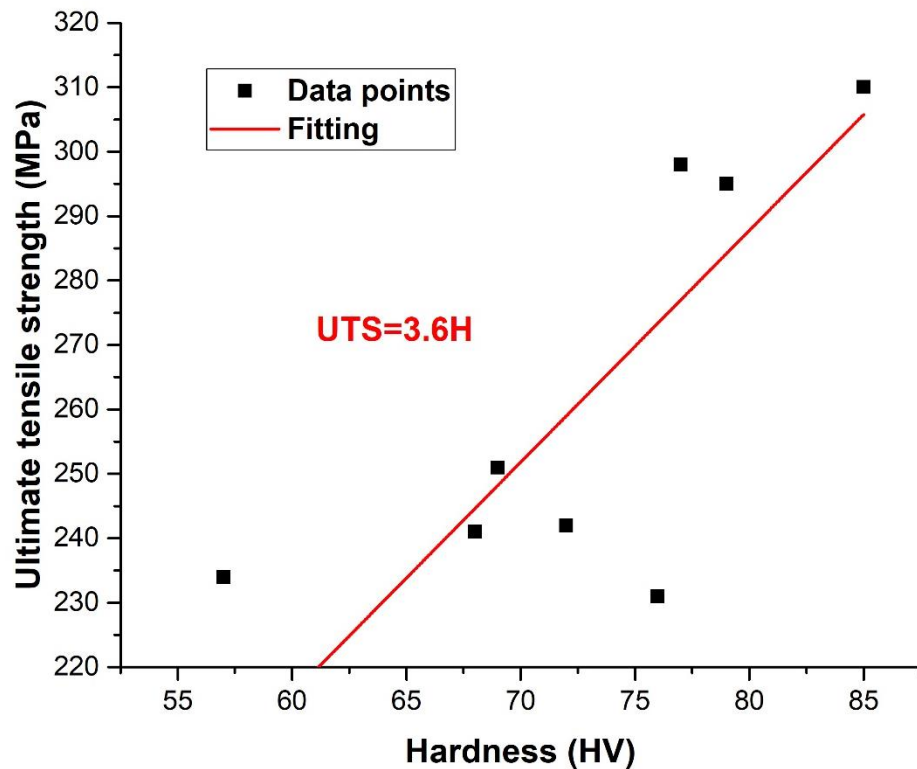
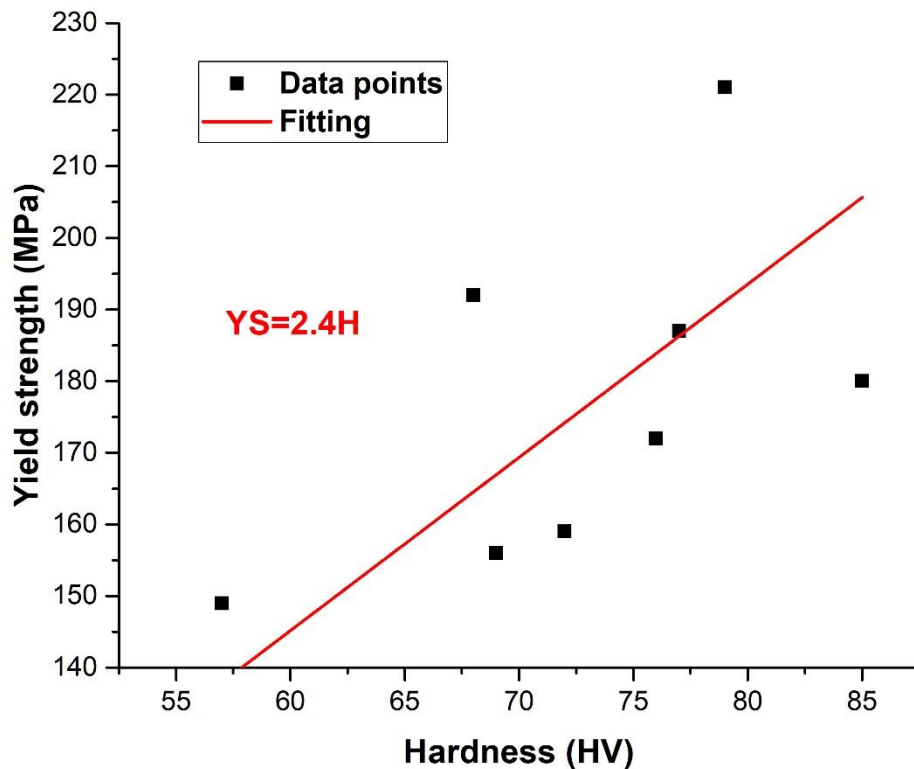


Figure 4.1a UTS vs HV between AA6061- AA5083 FSW welded joints

The graphs represent Hardness vs strength, where Hardness (HV) is on the X-axis and Ultimate Tensile Strength and Yield Strength are on the Y-axis. As this is a dissimilar welded joint, the points plotted are scattered very much likely, and the fitting data line might only cover some of the points in the graph due to dissimilarity in the composition of the alloys made. The UTS constant is 3.6H & YS constant is 2.4H.



**Figure 4.1b YS vs HV graph of AA6061-AA5083 welded joints.**

From Table 4.1, We can say that when the Rotational Speed is kept constant and the Transverse Speed is changed, Weld's hardness value and yield strength are gradually increased, whereas, On the Other Hand, the Ultimate Tensile Strength got reduced slowly. And when the transverse speed is kept constant, the rotational speed is changed then both ultimate tensile strength and hardness values decline gradually.

When this data is depicted in graphs ( UTS vs HV) and (YS vs HV), we can observe that the plotted points are scattered all across the space; this is because of hardness ( which is local strength ) which is taken uniformly along the two joints linearly. Two joints made of two dissimilar alloys, so when taken linearly, local strength is non-uniform, so points are scattered

all along the space, and the fitting data line appears in the middle of the space, not touching not more than one point clearly showing that there's non-uniformity in Hardness and Strength in the Friction Stir Welded Joint of 2 dissimilar Al alloys.

#### 4.3.2 Results obtained from Dissimilar AA6061-5083 FSW weld( case 2)

**Table 4.2 UTS vs YS vs HV values obtained from AA6061-5083 welded joints**

	YS[MPa]	UTS[MPa]	Hardness[HV]
AA5083	180	310	85
AA6061	221	295	79
700-40	140	185	81
700-60	167	224	79
700-80	176	229	83

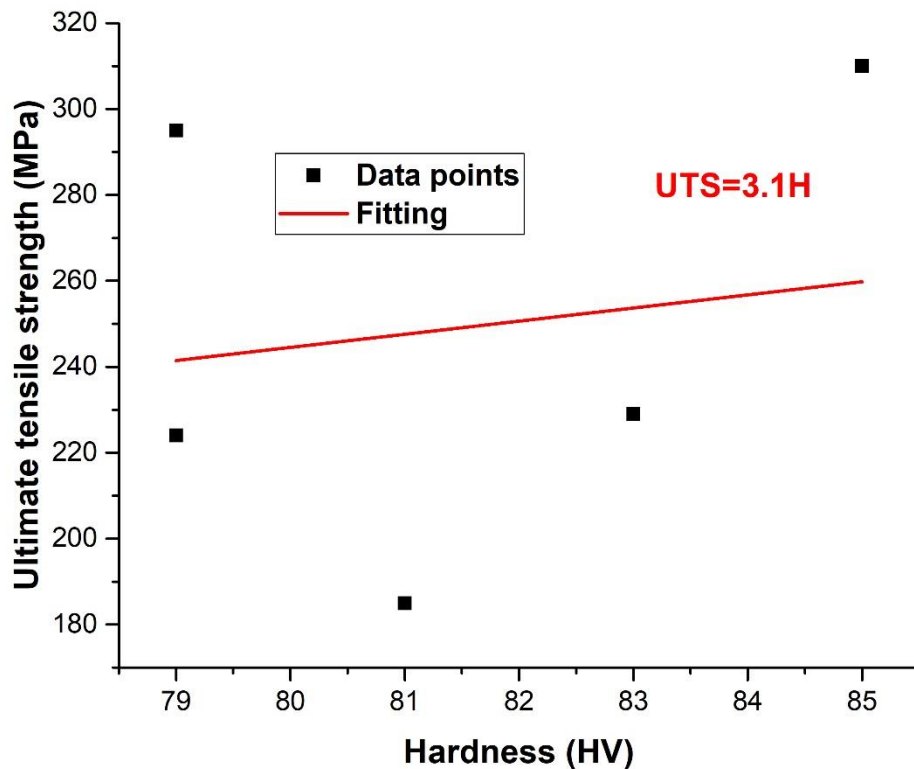


**Figure 4.2a UTS vs HV graph of AA6061-5083 welded joints.**

The graphs are a representation of local vs global strengths across the FSW welded joints, where hardness (HV) is on the X-axis, and Ultimate Tensile Strength( UTS) and Yield Strength (YS) are on the Y-axis. Similar to previous case 1, all the plotted points are scattered in space very much, and the fitting data line might only connect some of the points because of different microstructure compositions. Hence different hardness values are observed.

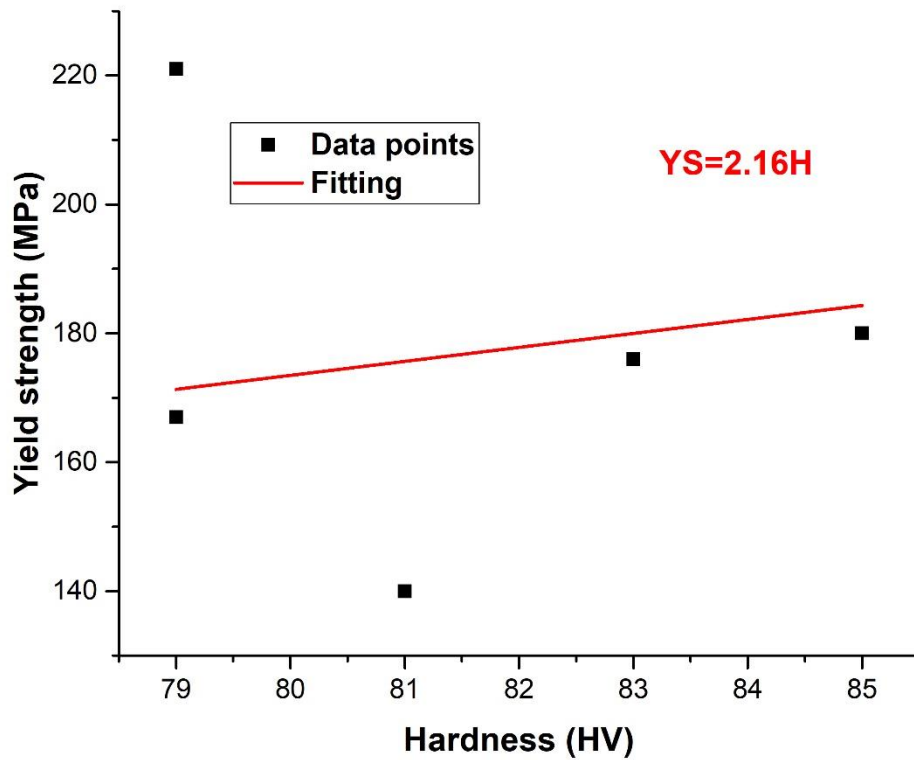


**Figure 4.2b YS vs HV graph of AA6061-5083 welded joints.**

Table 4.2 shows that the rotational speed is kept steady, the transverse speed of 20 is controlled and added, and the following results are tabulated. From the data, base metal ultimate tensile strength and hardness values are better-produced results than combined (dissimilar alloys) welded joints. When the transverse speed is added by the value 20, you can observe that Ultimate Tensile Strength and Yield Strength values grew, and the Hardness value didn't show any trend.

When the graph is prepared using Originpro software, the same results as before the case study is showcased: plotted points are scattered all over the space, and the fitting data line is not near

plotted points. The Data fitting line constants are of values 3.1H in UTS vs HV and 2.16H in YS vs HV graphs. Here also, the same phenomenon is considered: the presence of different metal compositions makes the non-uniformity in the result values. The resulting lines are not so steep but not so lean, and there's a gradual inclination to the fitting data line.

#### 4.3.3 Results Obtained from Similar AA6061 FSW Joint

**Table 4.3 UTS vs YS vs HV values obtained from Similar AA6061 welded joints**

	YS[MPa]	UTS[MPa]	Hardness[HV]
AA6061	221	295	79
900-30	175	221	65
1100-30	191	245	71
1300-30	146	178	56
1500-30	121	121	42

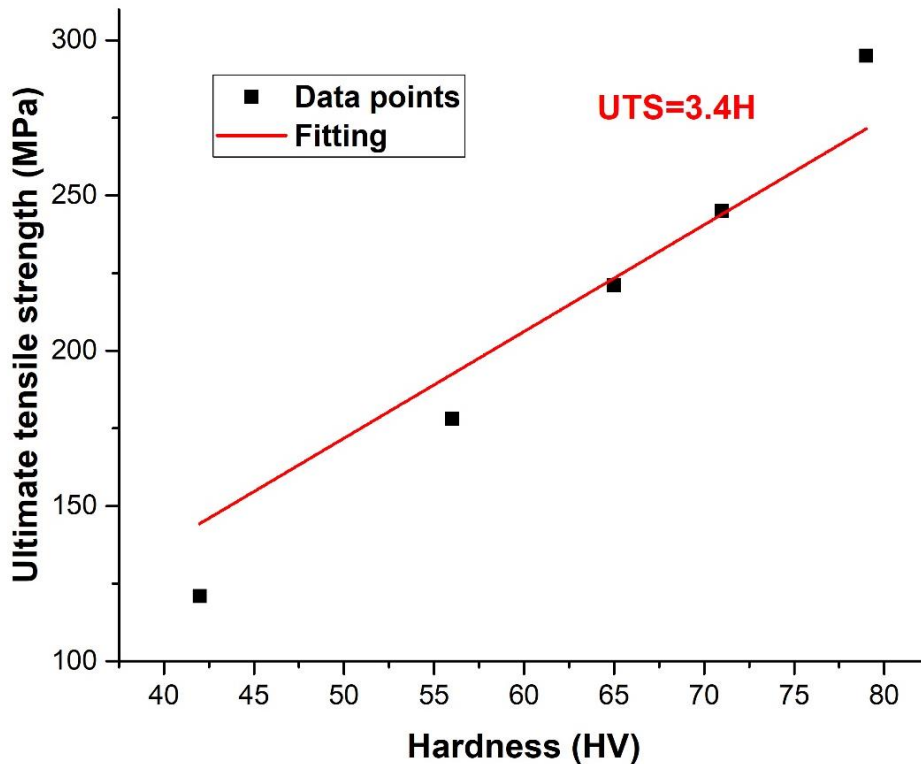


**Figure 4.3a UTS vs HV graph of AA6061 similar joints**

The graphs Figure 4.3a and Figure 4.3b represent Hardness(HV) on the x-axis with values ranging from 40-80 & Ultimate tensile strength(UTS) values ranging from 100-300, and Yield strength(YS) values ranging from 120-220 on the y-axis. Here plotted points are very close and appear nearer to the fitting data line because of the uniform composition of two similar metals, which makes the local and global strengths uniform across the joint. The fitting data line almost touches every plotted point. UTS constant value resulted in being 3.4H, and YS constant value was 2.7H.

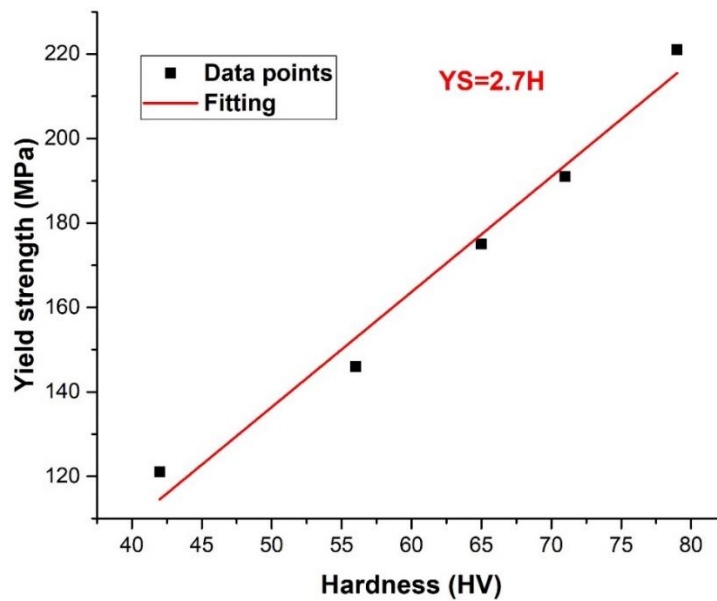


**Figure 4.3b YS vs HV graph of AA6061 similar joints**

From Table 4.3, the transverse speed is kept constant, and the rotational speed is increased at the rpm 200 for each weld. By observation, we clearly state that there's a surge in all three UTS, YS and HV values when the rotational speed is changed from 900 to 1100, and a linear decline in values is observed from 1300 rpm. This is why low rotational speed causes keyholes and tunnel defects in the weld because insufficient welding heat input results in insufficient plasticisation of the weld metal, which is inadequate to fill the cavity inside of the weld in the time driven by the mixing head. Therefore, increasing the spinning speed will ensure the weld heat input and encourage metal softening in the weld area, producing the production of a welded joint free from defects and deformation.

When data is represented in graphs, the fitting data line touches almost every point and appears closer to the plotted points than dissimilar joints. It means the hardness is uniform in all regions across the welded joint compared to dissimilar AA6061-5083 joints. The slope of both fitting data lines is uniform, not too steep or flat, and has a linear slope increase from start to end.

#### 4.4 Data collected from Similar Aluminium Alloy FSW welded joints

##### CASE 1:

**Table 4.4 UTS & HV values obtained from FSW of similar AA1200 with tapered tool[36]:**

UTS[MPa]	Hardness [HV]
73.6	36
89	37
79.5	38
71.6	35
85.4	37
76.23	36

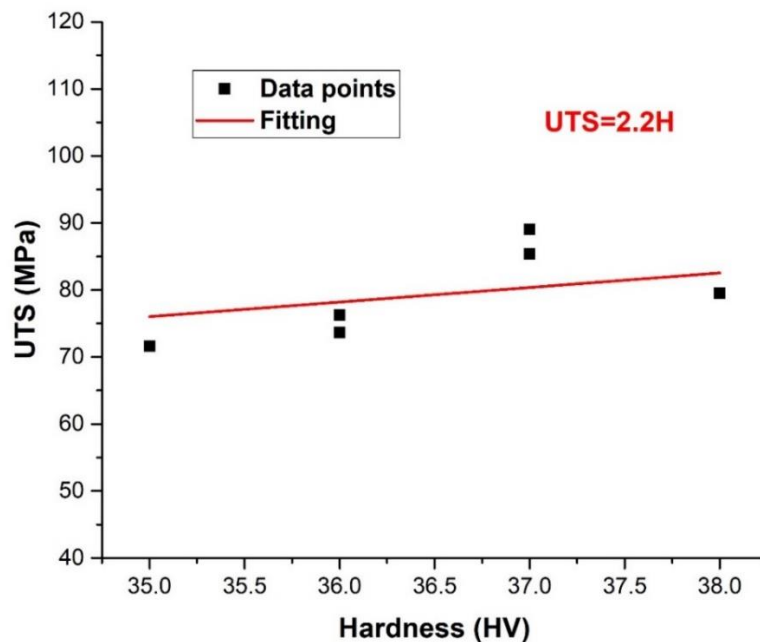


**Figure 4.4 UTS vs HV graph of AA1200 similar FSW welded joint**

**CASE 2:**

**Table 4.5 UTS vs HV values obtained from similar AA1200 FSW welded joint[36]**

UTS [MPa]	Hardness [HV]
70.19	34
83.23	36
74.68	35
85.41	37
76.23	36

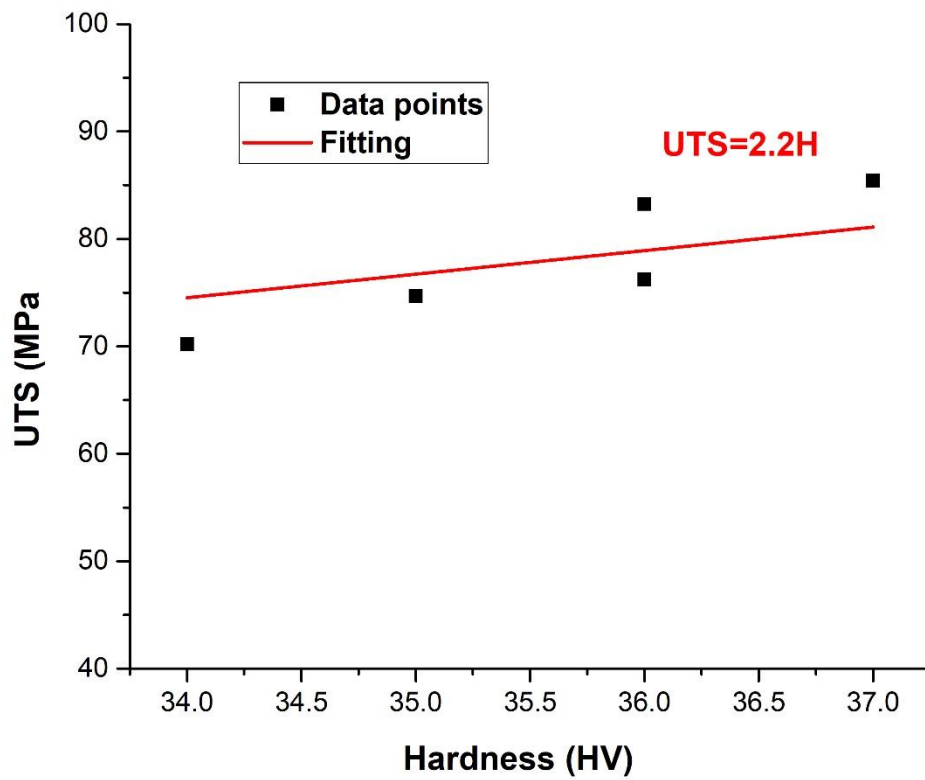


**Figure 4.5 UTS vs HV graph of similar AA1200 FSW welded joint.**



**CASE 3:**

**Table 4.6 UTS and HV values obtained from similar AA1200 FSW with a cylindrical tool with groove [36]**

UTS [MPa]	Hardness [HV]
70.31	34
80.4	37
75.35	36
69.31	34
79.5	37

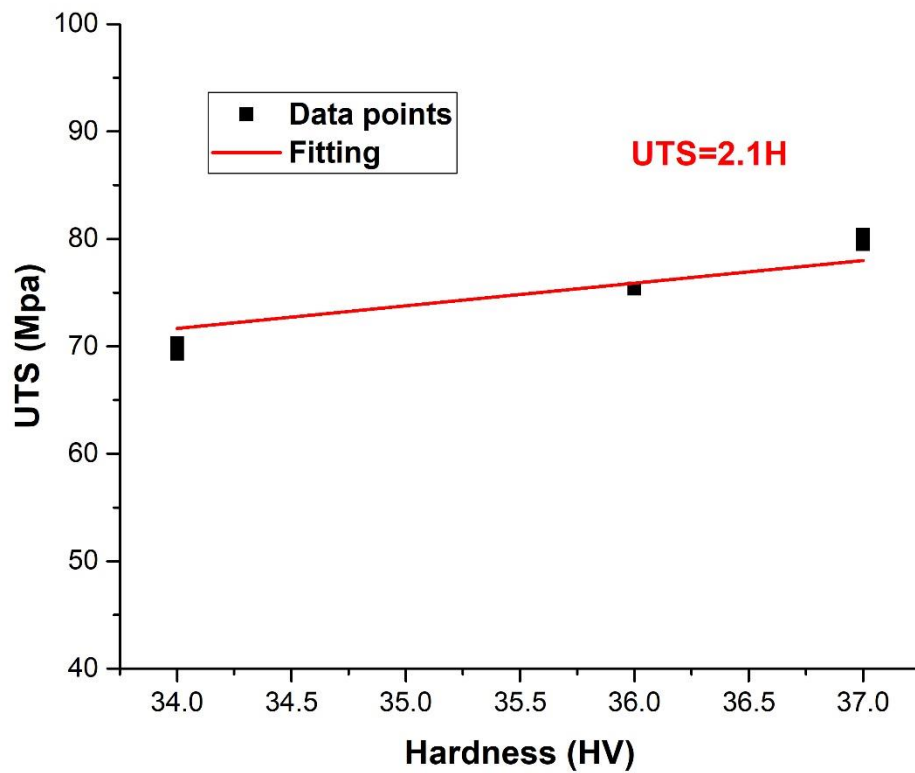


**Figure 4.6 UTS vs HV graph of similar AA1200 FSW weld joint with a cylindrical tool with groove**

**CASE 4:**

**Table 4.7 UTS vs HV values obtained from similar FSW joint [37]**

<b>UTS [MPa]</b>	<b>Hardness [HV]</b>
73.5	36
65.24	34
77.6	37
71.4	35
79.5	37

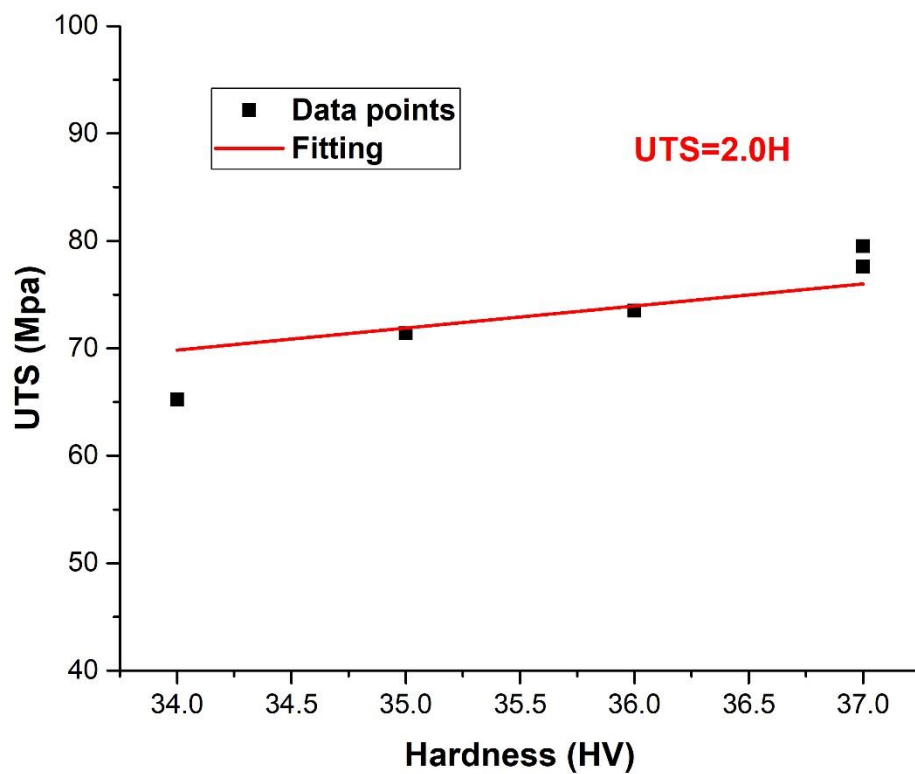


**Figure 4.7 UTS vs HV graph of similar FSW welded joint**

**CASE 5:**

**Table 4.8 UTS and HV values obtained from similar AA6061-T6 conventional FSW joint[38]**

UTS [MPa]	Hardness [HV]
85	185
108	185
92	182
95	189
114	199
109	191

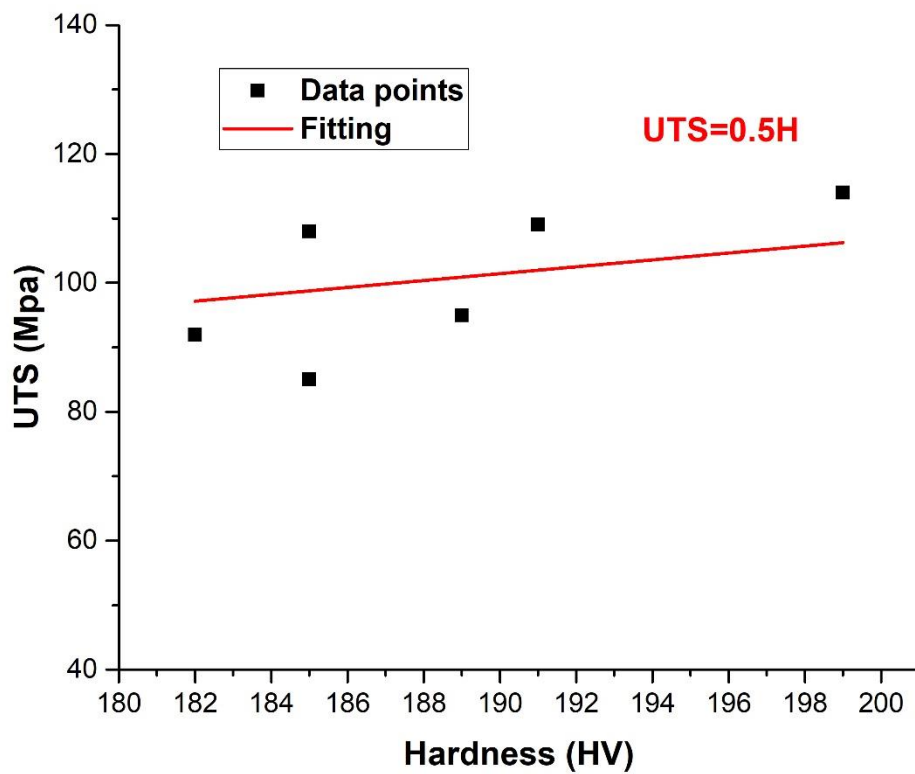


**Figure 4.8 UTS vs HV graph of similar AA6061-T6 FSW joint**

#### **4.4.1 Discussion**

The case studies focus on the welded joint material properties, such as tensile strength and hardness. Numerous research has been carried out to establish the effect of tool geometry on welded collective strength. Three FSW characteristics, including rotating tool speed, welding speed, and pin profiles, have been investigated for their implications on how the weld joint behaves mechanically. The results of the current study were used to illustrate how FSW's effects on parameters like hardness, tensile strength, and yield strength relate to the mechanical properties of welded joints.

One can infer that there is a strong bond formation during the formation of welding from the graphs that are being produced from case 1 to case 5 by gathering data because of the well-fitting data line from statistical values derived from literature studies of various authors who conducted friction experiments stir welding of related aluminium alloys.

For friction stir welding aluminium alloys under various processing circumstances, the Cahoon equation relations between hardness and strength (ultimate tensile strength and yield strength) are constructed based on equations (1) and (2), respectively. After applying the formulae, the data fit nicely.

#### 4.5 DATA OBTAINED FROM DISSIMILAR ALUMINIUM ALLOY FSW WELDS:

##### CASE 1:

Table 4.9 UTS vs HV values obtained from AA6061-T651 and AA7075-T651 FSW joint at 800rpm [39]

UTS [MPa]	Hardness [HV]
154	111.65
170	111.11
170	111.32
174	112.98
186	112.34

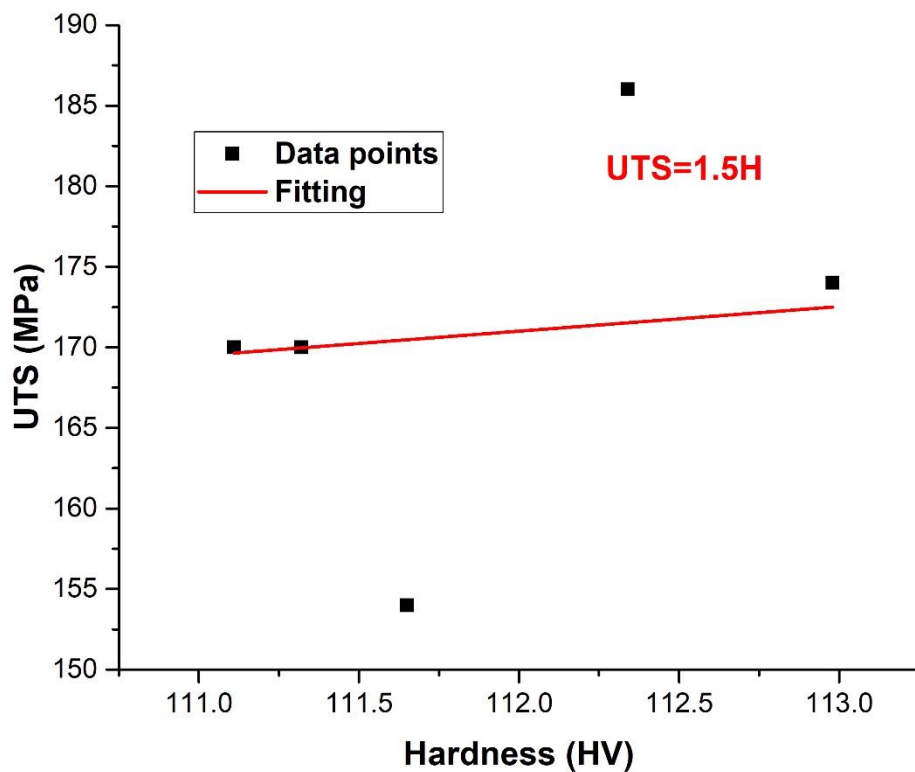
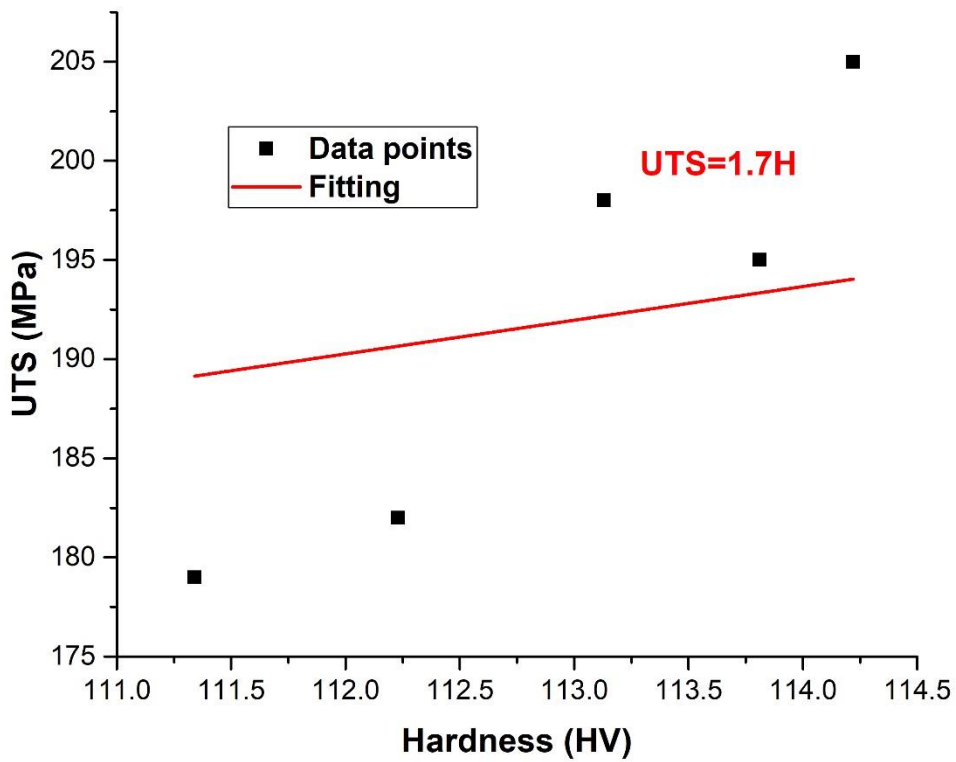


Figure 4.9 UTS Vs HV graph obtained from dissimilar AA6061-AA7075 FSW joint

**CASE 2:**

**Table 4.10 UTS vs HV values obtained from AA6061-AA7075 FSW joint at 900rpm [39]**

UTS [MPa]	Hardness [HV]
182	112.23
179	111.34
195	113.81
205	114.22
198	113.13



**Figure 4.10 UTS vs HV graph of dissimilar AA6061-AA7075 FSW joint**

**CASE 3:**

**Table 4.11 UTS and HV values obtained from AA6061 and AA7039 FSW joint [40]**

UTS [MPa]	Hardness [HV]
157	68.2
169	81.3
150	63.6
159	71.6
145	58.6
160	71.0
175	79.5

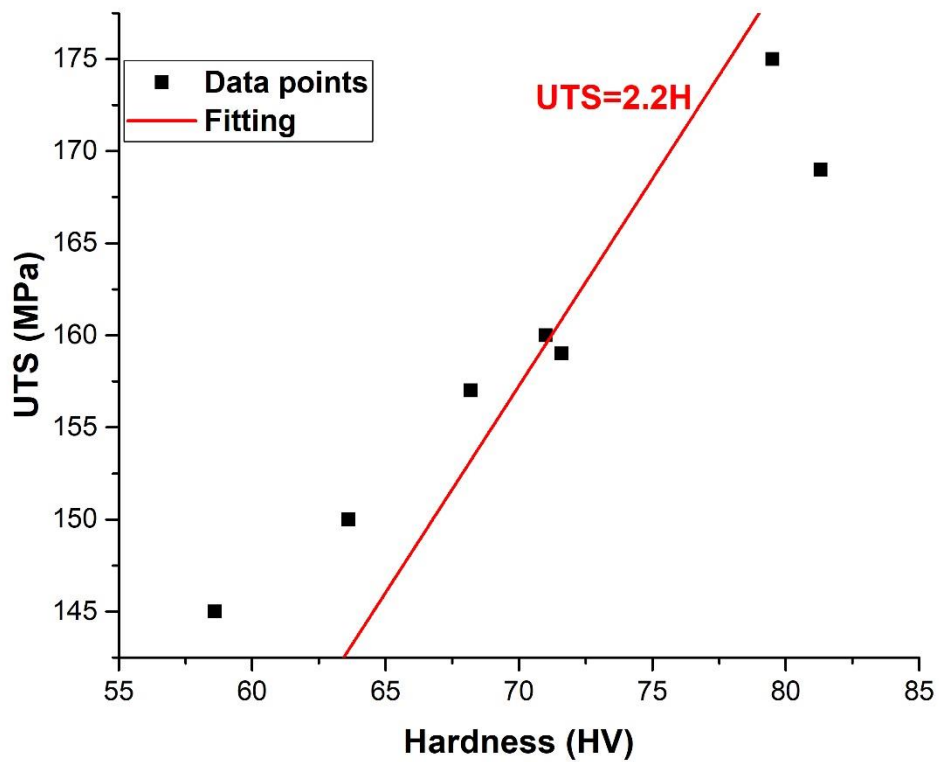


**Figure 4.11 UTS vs HV graph of dissimilar AA6061-7039 FSW joint**

**CASE 4:**

**Table 4.12 UTS and HV values obtained from AA2014-AA7075 FSW joint [41]**

UTS [MPa]	Hardness [HV]
325	45
346	49
314	47
306	42
338	49

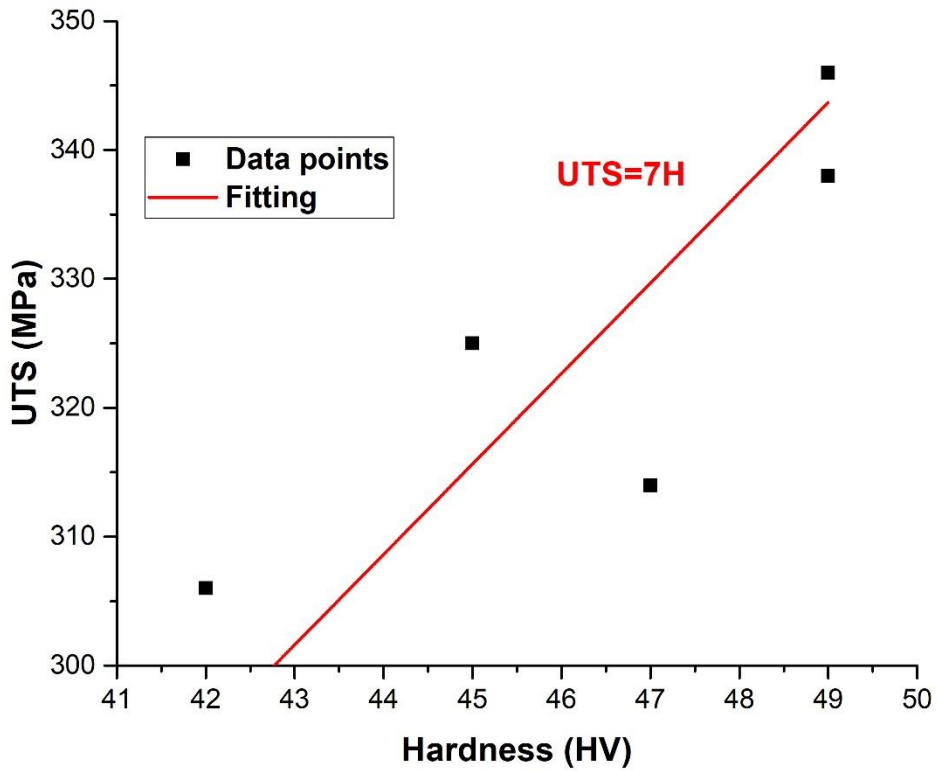


**Figure 4.12 UTS vs HV graph of dissimilar AA2014-AA7075 FSW joint**



**CASE 5:**

**Table 4.13 UTS and HV values Obtained from AA6061 T6-AA7075 T6 FSW joint [39]**

UTS [MPa]	Hardness [HV]
183	111.49
150	98.26
160	96.35
153	95.18
170	111.54

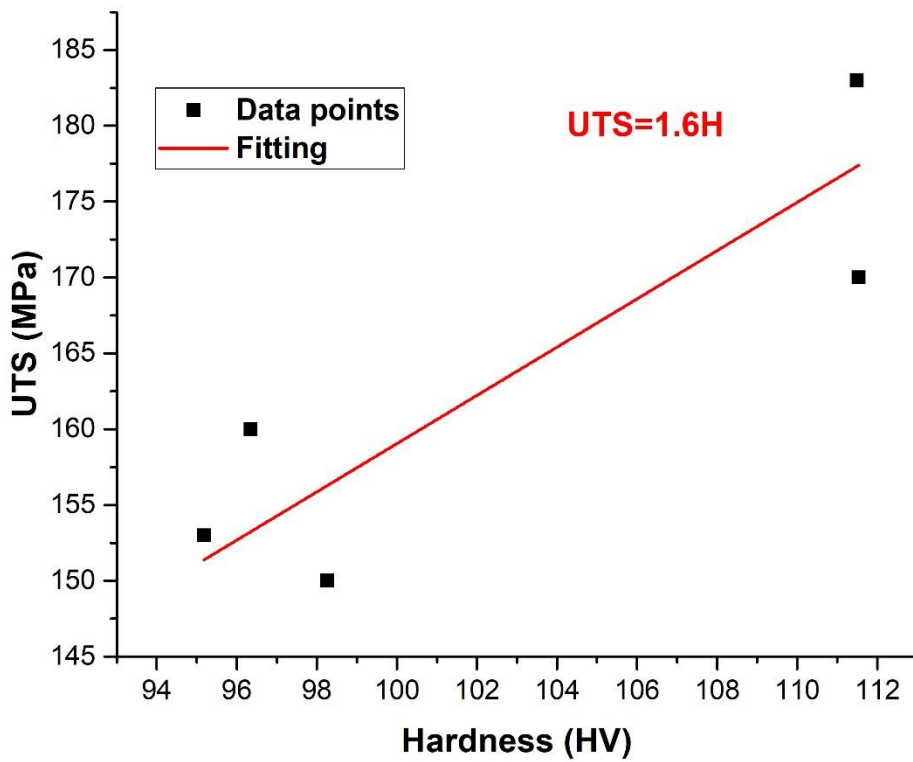


**Figure 4.13 UTS vs HV graph of dissimilar AA6061T6 – 7075T6 FSW joint**

### 4.5.1 Discussion

A dissimilar friction stir welded (FSW) joint graph commonly represents the change in the welded joint's mechanical characteristics. The graph's y-axis often reflects mechanical qualities, such as tensile strength and yield strength, while the x-axis typically represents the hardness of the welded junction.

The case studies involve friction stir welding of dissimilar aluminium alloys under precise conditions while tabulating mechanical parameters like yield strength, ultimate tensile strength, and hardness. The Cahoon equations (1) and (2), which establish the link between hardness and strength, are better understood considering the statistical data values acquired from literature studies. As you can see, the fitting data curve does not closely match the statistical data values. The data varied significantly.

The dissimilar FSW welded joint graphs, as a whole, offer valuable perceptions of the performance and quality of the welded junction, which can be used to establish the relationship between any two parameters. The friction stir welded joint's non-uniform composition, which results in varying tensile strengths and hardness at different points inside the same weld joint, prevents the Cahoon equation from being validated.

**4.6 Results obtained from composite welded joints:**

**CASE 1:**

**Table 4.14 UTS, YS, HV values obtained from 6061-T6 alloy surface hybrid components[42]**

HARDNESS [HV]	UTS [MPa]	YIELD STRENGTH [MPa]
121	162	134
93	159	126
89	141	114
102	173	147
89	164	137
96	145	120
92	197	163
107	126	95
95	149	119
102	285	263

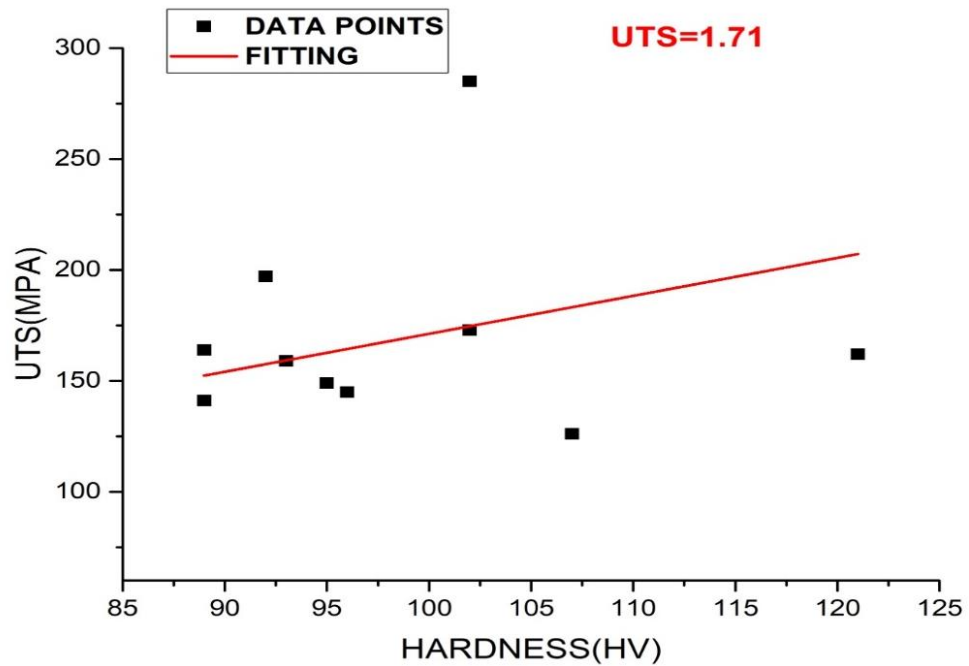


**Figure 4.14 UTS vs HV graph of composite welded joint of similar AA6061 FSW joints**

**CASE 2 :**

**Table 4.15 UTS YS HV values obtained from aluminium composites via friction stir welding[43]**

HARDNESS[HV]	UTS[MPa]	YIELD STRENGTH[MPa]
115	132	104
105	138	111
111	134	99
104	152	126
102	147	114
124	127	95
101	183	141
125	103	74
110	131	98
102	285	263

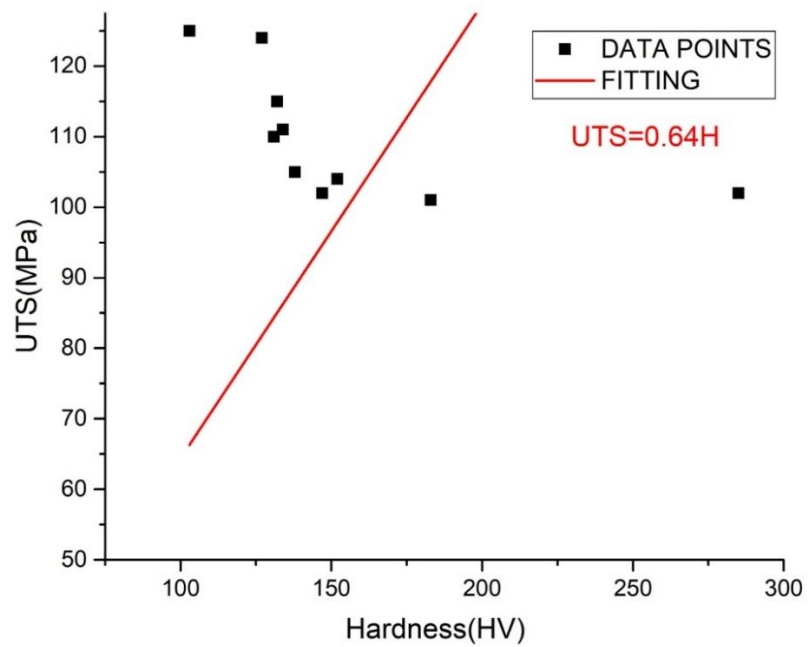


**Figure 4.15 UTS vs HV graph of aluminium composites via FSW**

**CASE 3:**

**Table 4.16 UTS HV values obtained from composite reinforced FSW joint[44]**

<b>HARDNESS [HV]</b>	<b>UTS [MPa]</b>
111.4	270
122.4	277.3
117.3	269.7
122.3	268
124.4	189
66	230

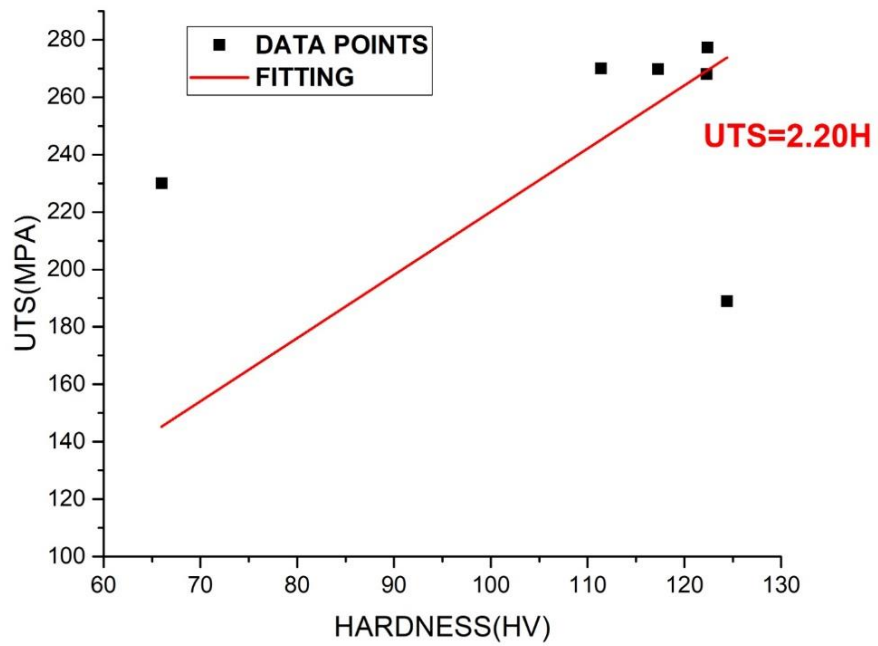


**Figure 4.16 UTS vs HV graphs of composite reinforced FSW joint**

**CASE 4:**

**Table 4.17 UTS HV values obtained from aluminium composites FSW joint[45]**

Hardness [HV]	UTS [MPa]
108.3	263
112.3	244
114.8	250
112.9	262
111.4	270
110	274
113.9	190.7

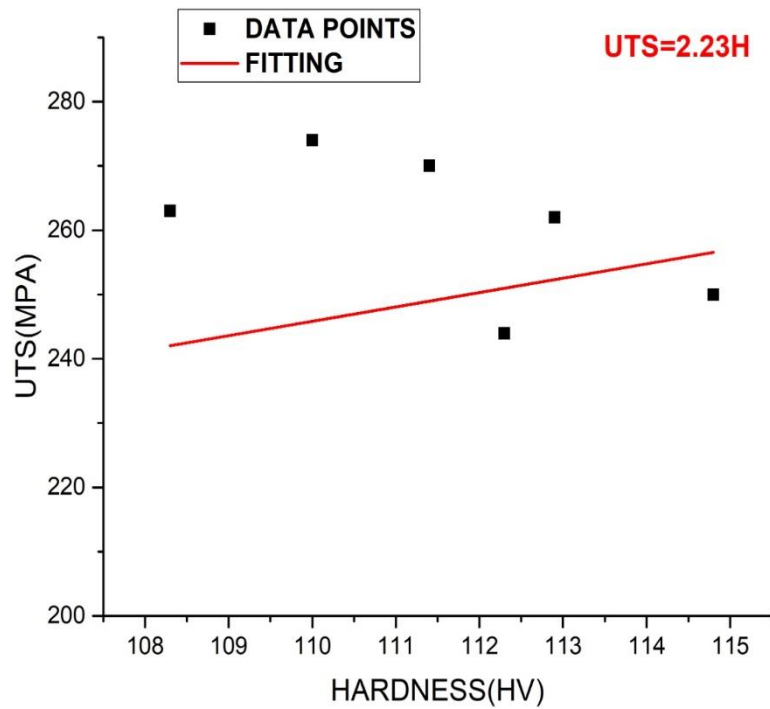


**Figure 4.17 UTS vs HV graph of aluminium composites FSW joint**

**CASE 5:**

**Table 4.18 UTS YS HV values obtained from surface hybrid AL composites[46]**

UTS [MPa]	Hardness [HV]	YS [MPa]
84.6	37.4	49.7
64.8	71.1	41.5
96	65.7	45.8
64.8	56.1	32.5
76.7	50.2	51.3
90.6	50.5	55.1

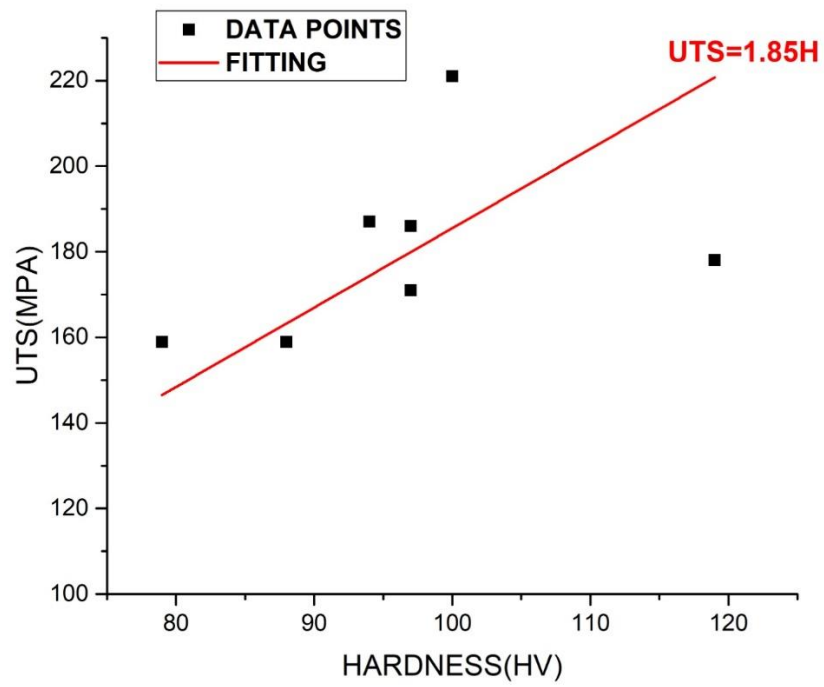


**Figure 4.18 UTS vs HV graph of surface hybrid aluminium composites**

#### 4.6.1 Discussion

Similar research was done on the reinforced composites that FSW produced. The authors created the aluminium alloy composites using FSW, and statistical information about those composites, including their Hardness and tensile strength, was described in Tables 4.14 to 4.18. The authors developed equations (1) and (2) using the information from these tables to build a link between hardness and strength (YS and UTS). The created graphs revealed that the well-known associations for reinforced composites made by FSW appear implausible. The investigational results could have matched the established equations better.

The statistical data for the UTS versus H instance varied greatly. It is well recognised that reinforcing agent type, size, and quantity—rather than matrix particle size—significantly impact the hardness and strength of composite materials. The presence of reinforcing compounds causes the hardness of composites made by FSW not to be homogeneous and to vary significantly over the SZ. In addition, the supporting agents change the tensile strength of composites, which scatters experimental data. Thus, it was determined that because of surface heterogeneity and aggregation of reinforcing chemicals, it is impossible to create a relationship between Hardness (HV) and Strength for composites made by FSW.

The authors additionally summarised the friction stir modified and strengthened aluminium alloy information from the literature revisions to authenticate the equations. Hardness, yield strength, and ultimate tensile strength information from the literature were recorded. It was measured and reported what the constants were between hardness and strengths. It was determined that the experimental data for friction stir welded alloys agreed with equations (1) and (2). Instead, the patterns of composites created by FSW appeared to be more complex, which resulted in an erroneous assessment of the constants relating hardness to strength. Finally, it was determined that developing a uniform fine-grained structure makes it imaginable to construct a linear bond between the hardness and strength of FSW aluminium alloys.



## CHAPTER 5

### CONCLUSION

Through experimental inquiry and literature research, this project sought to establish a link between friction stir welding joints made of an aluminium alloy and its hardness and strength. The following criteria were outlined during the search :

- By observing Experimental data, the dissimilar AA6061-AA5083 FSW joint graphs of UTS vs HV and YS vs HV, the fitting data line does not fit very well (i.e., not touching the plotted points) because of non-homogeneity of the composition of microstructures.
- By observing the experimental data, the similar AA6061 FSW joint graphs of UTS vs HV and YS vs HV, the fitting data line does fit very well ( i.e., almost touching every plotted point) because of homogeneity in the composition of microstructures.
- Based on the statistical analysis found that the homogenous weld zone generation was responsible for the comparable FSW welding joint experimental data fitting well with the stated equations.
- Due to producing a non-homogenous weld zone, statistical data shows that the experimental data from the dissimilar FSW welding joint does not fit well with established equations.
- Lastly, the analysis of experimental results and data from the literature showed no relationship between the hardness and strength of friction stir processed reinforced composites. This is principally because of physical non-homogeneity from the reinforcing agents' type, size, and volume. The current study will optimise the optimum overlapping balance grounded on the top investigational fit, which results in the homogeneous treated zone for a vast region of stir zone manufactured by FSW employing pin imbrication with various overlying ratios.

## CHAPTER 6

### REFERENCES

1. **Thomas et al. (1991)** of The Welding Institute (TWI).
2. **Lohwasser (2009)** suggested that two types of material flows are possible in FSW: pin-driven and shoulder-driven.
3. **Cavaliere et al. (2006)** investigated the tensile and fatigue behaviour of 2024 and 7075 alloys FSW.
4. **Sundaram et al. (2010)** analysed the friction stir welding for AA2024-T6 and AA5083-H321 using five different pin profiles.
5. **Leitao et al. (2009)** studied mechanical behaviour on dissimilar joints of AA5182-H111 and AA60616-T4.
6. **El Rayes, M.M., Soliman, M.S., Abbas, A.T., Pimenov, D.Y., Erdakov, L.N., Abdel-Mawla, M.M., 2019.** Effect of feed rate in FSW on the mechanical and microstructural properties of AA5754 joints. *Adv. Mater. Sci. Eng...*
7. **El-Sayed, M.M., Shash, A.Y., Mahmoud, T.S., Abd-Rabbou, M., 2018a.** Effect of friction stir welding parameters on the peak temperature and the mechanical properties of aluminium alloy 5083-0. *Adv. Struct. Mater.* 72, 11-25
8. **PALANIVEL R, DINAHARAN I, LAUBSCHER R F.** Casting routes to produce metallic-based composite parts [M]//Encyclopaedia of materials: Composites. Elsevier, 2020. DOI:10.1016/B978-0-12-803581-8.11882-X.
9. **MOFID M A, ABDOLLAH-ZADEH A, GHAINI F M.** The effect of water cooling during dissimilar friction stir welding of Al alloy to Mg alloy [J]. *Materials & Design*, 2012, 36: 161–167.
10. **MOFID M A, ABDOLLAH-ZADEH A, GHAINI F M, GÜR C H.** Submerged friction-stir welding (SFSW) underwater and under liquid nitrogen: an improved method to join Al alloys to Mg alloys [J]. *Metallurgical and Materials Transactions A*, 2012, 43: 5106–5114.
11. **SUNDARAM N S, MURUGAN N.** Tensile behaviour of dissimilar friction stir welded joints of aluminium alloys [J]. *Materials & Design*, 2010, 31: 4184–4193
12. **A. Steuwer, M. J. Peel, and P. J. Withers,** Dissimilar friction stir welds in AA5083-AA6082: The effect of process parameters on residual stress, *Mater. Sci. Eng. A* 441, 187–196 (2006).

13. **M. J. Peel, A. Steuwer, P. J. Withers, T. Dickerson, Q. Shi, and H. Shercliff,** Dissimilar friction stir welds in AA5083-AA6082. Part I process parameter effects on thermal history and weld properties, *Metall. Mater. Trans. A* 37A, 2183–2193 (2006).
14. **M. P. Miles, D. W. Melton, and T. W. Nelson,** Formability of friction-stir-welded dissimilar-aluminium-alloy sheets, *Metall. Mater. Trans. A* 36A, 3335–3342 (2005).
15. **Mohammad HasanShojaeefarda, Reza AbdiBehnaghb, Mostafa Akbari, Mohammad KazemBesharatiGivi, FoadFarhani. and Pareto** Modelling optimisation of mechanical properties of friction stir welded AA7075/AA5083 butt joints using neural network and particle swarm algorithm [J]. *Materials and Design*, 2013,44:190–198.
16. **Shah, LH., Guo, S., Walbridge, S., Gerlich, A.P., 2017.** Effect of tool eccentricity on the properties of friction stir welded AA6061 aluminium alloys. *Manuf. Lett.* 15, 14-17.
17. **Abdulstaar, M.A., Al-fadhalah, K.J., Wagner, L., 2017.** Microstructural variation through weld thickness and mechanical properties of peened friction stir welded 6061 aluminium alloy joints. *Mater. Charact.* 126, 64-73.
18. **K.P. Yuvaraj, P. AshokaVarthanan, L. Haribabu, R. Madhubalan, K.P. Boopathiraja.** Optimisation of FSW tool parameters for joining dissimilar AA7075-T651 and AA6061 aluminium alloys using Taguchi Technique, *Mater. Today: Proc*, 2020.
19. **SADEESH P, KANNAN M V, RAJKUMAR V, AVINASH P, ARIVAZHAGAN N, RAMKUMAR K D, NARAYANAN S.** Studies on friction stir welding of AA 2024 and AA 6061 dissimilar metals [J]. *Procedia Engineering*, 2014, 75: 145–149
20. **MAHTO R P, GUPTA C, KINJAWADEKAR M, MEENA A, PAL S K.** Weldability of AA6061-T6 and AISI 304 by underwater friction stir welding [J]. *Journal of Manufacturing Processes*, 2019, 38: 370–86.
21. **Y. Li, L. E. Murr, and J. C. McClure,** Solid-state flow visualisation in the friction-stir welding of 2024 Al to 6061 Al, *Scripta Mater.* 40, 1041–1046 (1999)
22. **Y. Li, L. E. Murr, and J. C. McClure,** Flow visualisation and residual microstructures associated with the friction stir welding of 2024 aluminium to 6061 aluminium, *Mater. Sci. Eng. A* A271, 213–223 (1999)

23. **C. Rathinasuriyan, V. S. Senthil Kumar.** Modelling and optimisation of submerged friction stir welding parameters for AA6061-T6 alloy using RSM [J]. *Kovove Mater*, 2016,54: 297–304
24. **Rajkumar S, Muralidharan C, Balasubramanian V.** Establishing empirical relationships to predict grain size and tensile strength of friction stir welded AA 6061-T6 aluminium alloy joints [J]. *Trans.NonferrousMet.Soc.China*, 2010,20:1863-1872.
25. **Prabhu, S.R.B., Shettigar, A.K., Herbert, M.A., Rao, S.S., 2019.** Microstructure evolution and mechanical properties of friction stir welded AA6061/Rutile composite. *Mater. Res. Express* 6 (8) 086517.
26. **Kalaiselvan, K., Dinaharan, I., Murugan, N., 2014,** Characterization of friction stir welded boron carbide particulate reinforced AA6061 aluminium alloy stir cast composite. *Mater. Des.* 55, 176-182.
27. **Re N, Ocheri C. Jc O, et al.** The empirical relationship between hardness and tensile strength for medium carbon steel is quenched in different media. *J Mater Sci Eng* 2019; 8: 1-5.
28. **Zhang P. Li SX and Zhang ZF** General relationship between strength and hardness. *Mater Sci Eng A* 2011; 529: 62-73.
29. **Pavlina EJ and Van Tyne CJ.** Correlation of Yield Strength and Tensile strength with hardness for steels. *J Mater Eng Perform* 2008; 17: 888-893.
30. **Lu W, Shi Y, Li X, et al.** Correlation between tensile strength and hardness of electron beam welded TC4- DT joints. *J Mater Eng Perform* 2013; 22: 1694-1700.
31. **CAVALIERE P, SQUILLACE A, PANELLA F.** Effect of welding parameters on mechanical and microstructural properties of AA6082 joints produced by friction stir welding [J]. *Journal of Materials Processing Technology*, 2008, 200: 364–372.
32. **GAŠKO M, ROSENBERG G.** Correlation between hardness and tensile properties in ultra-high strength dual phase steels [J]. *Materials Engineering*, 2011, 18: 155–159.
33. **SHEN Y L.** The correlation between hardness and tensile strength in particle-reinforced metal matrix composites [J]. *Materials Science and Engineering A*, 2001, 297: 44–47.
34. **CAHOON J R, BROUGHTON W H, KUTZAK A R.** The determination of yield strength from hardness measurements [J]. *Metallurgical Transactions*, 1971, 2: 1979–1983.

35. **CAHOON J R.** An improved equation relating hardness to ultimate strength [J]. Metallurgical Transactions, 1972.
36. **M. George Joseph, J. Shaji, M. Francis, A. Raghavan, K. Shunmugesh,** Measurement of Tensile Properties and Hardness of Friction Stir Welded Aluminium Alloy AA1200, Mater. Today: Proc. 24 (2020) 1987–1993
37. **El-Sayed, M.M., Shash, A.Y., Abd-Rabbou, M., 2018b.** Finite element modelling of aluminium alloy AA5083-0 friction stir welding process. J. Mater. Proc. Tech. 252, 13-24.
38. **Fathi J, Ebrahim Zadeh P, Farasati R, Teimouri R.** Friction stir welding of aluminium 6061-T6 in water cooling: analysing mechanical properties and residual stress distribution. Int J Light Mater Manuf 2019;2:107–15.
39. **S.Ravikumar, V. Seshagiri Rao and R.V. Pranesh,** "Effect of Process Parameters on Mechanical Properties of Friction Stir Welded Dissimilar Materials between AA6061-T651 and AA7075-T651 Alloys", International Journal of Advanced Mechanical Engineering, Vol. 4, 2014, pp. 101-114.
40. **Divya Deep Dhancholia, Anuj Sharma, Charit Vyas,** "Optimisation of Friction Stir Welding Parameters for AA 6061 and AA 7039 Aluminium Alloys by Response Surface Methodology (RSM)" Volume 4, Number 5(2014), pp.565-57.
41. **V. Saravanan, N. Banerjee, R. Amuthakkannan, S. Rajakumar,** Microstructural evolution and mechanical properties of friction stir welded dissimilar AA2014-T6 and AA7075-T6 aluminium alloy joints, Metallography, Microstructure, and Analysis. 4 (3) (2015) 178–187.
42. **Devaraju, A. Kumar, B. Kotiveerachari** "Influence of rotational speed and reinforcements on wear and mechanical properties of aluminium hybrid composites via friction stir processing" Materials and Design 45 (2013) 576–585.
43. **Devaraju, A., Kumar, A., Kumaraswamy, A., Kotiveerachari, B.,** Influence of Reinforcements (SiC&Al<sub>2</sub>O<sub>3</sub>) and Rotational speed on Wear and Mechanical Properties of Aluminium alloy 6061T6 based Surface Hybrid Composites produced via Friction stir processing, Materials and Design (2013).
44. **M.Bahrami, M.K.Besharati Givi, K. Dehghani, and N. Parvin,** "On the role of pin geometry in microstructure and mechanical properties of AA7075/SiC nano-composite fabricated by friction stir welding technique", Mater. Des. 53, pp. 519 – 527, 2014.

45. **Bahrami, M., Dehghani, K., Givi, M.K.B.,** A novel approach to developing aluminium matrix nano-composite employing friction stir welding technique, *Materials and Design* (2013).
46. **Khodabakhshi F, Simchi A, Kokabi AH, Nosko M, Simancik F, Svec P.** Microstructure and texture development during friction stir processing of Al-Mg alloy sheets with TiO<sub>2</sub> nanoparticles. *Mater Sci Eng*, 2014;605:108-16.